Abstract

Alkaline wastes have been the focus of many studies as they act as CO_2 sinks and have the potential to offset emissions from mining and steelmaking industries. Passive carbonation of alkaline wastes mimics natural silicate weathering and provides a promising alternative pathway for CO_2 capture and storage as carbonates, requiring marginal human intervention when compared to ex-situ carbonation. This review summarizes the extant research that has investigated the passive carbonation of alkaline wastes, namely ironmaking and steelmaking slag, mine tailings and demolition wastes, over the past two decades. Here we report different factors that affect passive carbonation to address challenges that this process faces and to identify possible solutions. We identify avenues for future research such as investigating how passive carbonation affects the surrounding environment through interaction with the biosphere and the hydrosphere. Future research should also consider economic analyses to provide investors with an in-depth understanding of passive carbonation techniques. Based on the reviewed materials, we conclude that passive carbonation can be an important contributor to climate change mitigation strategies, and its potential can be intensified by applying simple waste management practices.

Keywords: Carbon sequestration; mineral carbonation; slag; tailings; artificial soil; silicate weathering.

1. Introduction

The United Nations Statistics Department (UNSD) defines wastes as substances that are not primary products (produced for the market) and are meant to be disposed of as the generators have no use for them in consumption, production, and transformation (UNSD, 2016). Several industries generate wastes of alkaline nature. For example, ironmaking and steelmaking produce slag, aluminium production produces red mud, mining operations produce tailings and buildings demolition produces demolition wastes (Renforth, 2019). The alkaline nature of these wastes is attributed to their content of alkaline earth oxides, notably calcium oxide (CaO) and magnesium oxide (MgO); both can hydrate to produce $Ca(OH)_2$ and $Mg(OH)_2$, respectively, which act as alkalinity sources (Riley and Mayes, 2015; Roadcap et al., 2006, 2005). High pH is associated with several leachates from alkaline residues (Mayes et al., 2006; Meyer, 1980). Such leachates cause several environmental problems like smothering of littoral aquatic habitats and reduction of light penetration to benthic producers (Mayes et al., 2008a). Leachates also contain metals at concentrations that are harmful to macrophytes and other organisms in the food web and can cause contamination of drinking water sources and agricultural land pollution (Gao et al., 2021; Olszewska et al., 2016). Alkaline wastes can contain high concentrations of ecotoxic metals such as lead and chromium (VI) which can reach 978 mg/kg and 851 mg/kg, respectively (Hu et al., 2020). Such metals can be released into the environment as a result of infiltration by rain or other water sources (Gomes et al., 2016; Mayes et al., 2011).

Historically, alkaline wastes have been either abandoned near production sites or collected into storage facilities (Riley et al., 2020; Santini and Banning, 2016). Recently, due to the increased awareness of sustainability and the drive towards a

circular economy, there have been several attempts to utilize alkaline wastes, particularly in road construction, land restoration, element recovery and more recently in carbon capture and sequestration (CCS) (Gomes et al., 2016; Santini and Banning, 2016; Sorlini et al., 2012). The latter idea gained considerable attention as it mimics natural weathering (Kelemen et al., 2020, 2011; National Academies of Sciences Engineering and Medicine, 2019). Natural silicate weathering and subsequent carbonate precipitation are critical processes that control the atmospheric CO_2 concentration (Daval, 2018; Huh, 2003; Schuiling and Krijgsman, 2006). This process captures carbon at a rate of 1-2.8 g C m^{-2} y^{-1} while mineral carbonation of alkaline wastes captures carbon at rates that are orders of magnitude greater than this value (Amiotte Suchet et al., 2003; Gaillardet et al., 1999; Huh, 2003; Oskierski et al., 2013; Wilson et al., 2014).

The high production of metals throughout the world (Fig. 1) results in vast amounts of alkaline wastes, which was estimated to be produced at an annual rate of 7 x 10^{12} - 1.7 x 10^{13} kg y^{-1} globally and projected to increase during this century (Renforth et al., 2011; Renforth, 2019). Power et al. (2013) estimated that ultramafic wastes can capture up to 1.75 x 10^{11} kg CO_2 y^{-1}, while Renforth et al. (2011b) estimated a CO_2 uptake potential of 7.0 x 10^{11} kg CO_2 y^{-1} when considering other alkalinity sources such as demolition wastes and slag. Renforth (2019) calculated that CO_2 emissions associated with different shared socioeconomic pathways and showed that by 2100, the CO_2 emissions are projected to be between 2.4 x 10^{13} kg CO_2 y^{-1} and 1.26 x 10^{14} kg CO_2 y^{-1}, and alkaline wastes carbonation can mitigate between 5% and 12% of these emissions. Carbonation of wastes has also been associated with reducing their environmental hazards since it reduces the pH of leachates as well as the concentration of metals in leachates, though the latter was found to depend on the

degree of carbonation (Gomes et al., 2016; Van Gerven et al., 2006). As CO_2 mineralisation can offset the emissions of mining and steelmaking industries, it can result in several economic, societal and biological benefits that are aligned with different sustainable development goals, including good health and well-being, climate action, sustainable cities and communities and quality of life on land (Olabi et al., 2022).

The Intergovernmental Panel on Climate Change (IPCC) explains that to avoid catastrophic consequences of global warming, the global temperature must not increase by more than 1.5 °C by the end of this century, compared to the preindustrial period (1850-1900) (IPCC, 2021). Here, we study the opportunities and challenges of using passive carbonation as a simple and inexpensive climate change mitigation pathway. This paper is structured as follows: Section 2 describes the carbonation reactions, including how different conditions can affect the CO_2 uptake; Section 3 reviews relevant studies of passive carbonation in slag, demolition wastes and tailings. We focus on slag, construction and demolition wastes, nickel tailings, chrysotile tailing, diamond tailings and red mud. Large stocks of these materials are available worldwide, and except for chrysotile, these materials are produced in large amounts. These wastes have been passively managed for a period long enough to allow for passive carbonation to be observed. Additionally, they have favorable chemistry that enables them to offset emissions of mining and steelmaking industries (Bullock et al., 2022). Section 4 summarizes some limitations that reduce CO_2 uptake in alkaline wastes, and Section 5 suggests some large-scale methods that can utilize passive carbonation. Based on our engagement with the studied articles, we propose several areas of further research, particularly related to life cycle assessment, economic

95 analysis and the relation of passive carbonation to the surrounding environment.
96 These areas are discussed in Section 6.

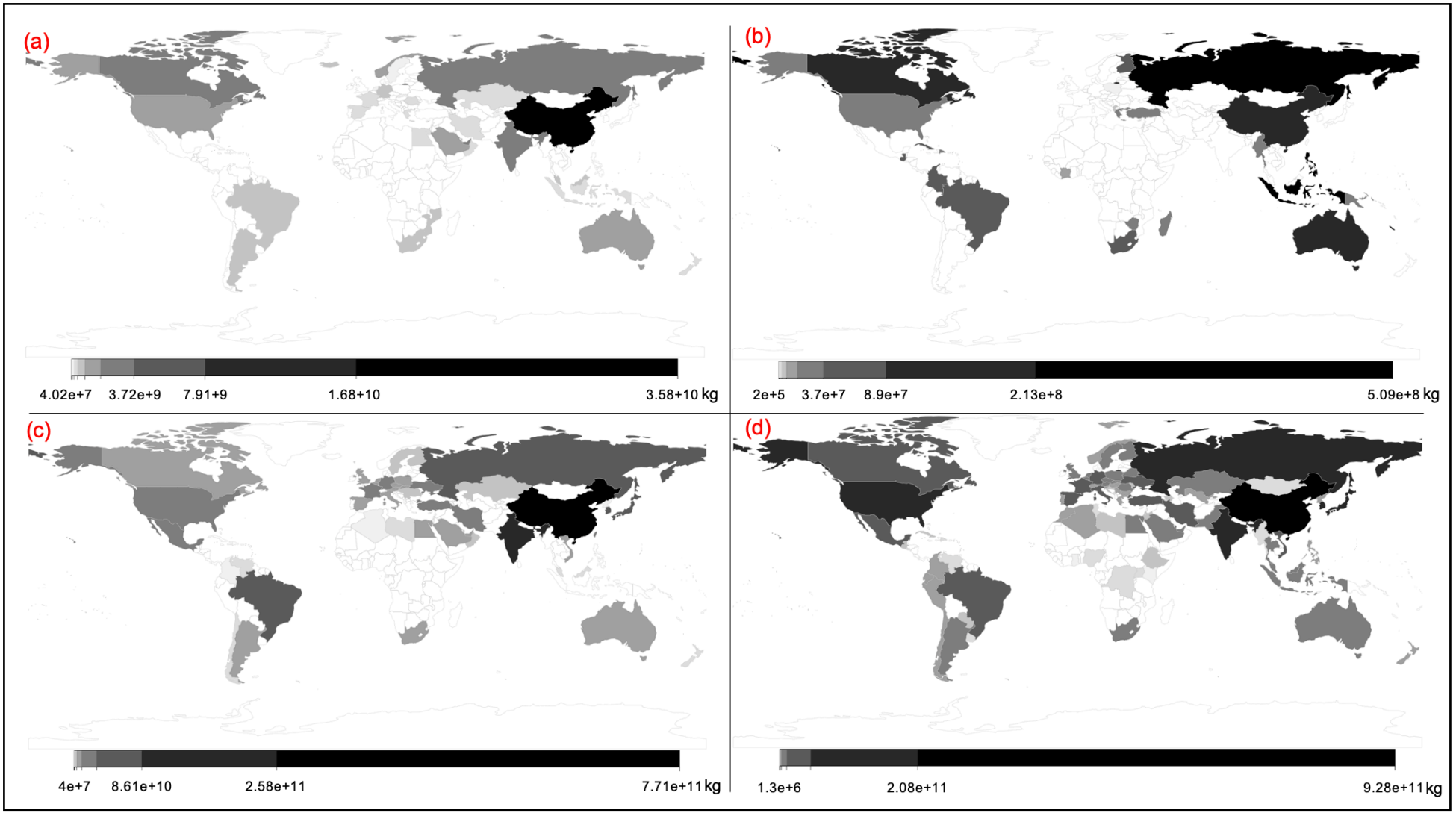

Fig. 1. Production (in kg) of (a) primary aluminum, (b) nickel, (c) pig iron, and (d) crude steel in 2018. White areas represent countries for which data were not available. Data from World Mineral Statistics contributed by permission of the British Geological Survey (Brown et al., 2020).

2. Mineral carbonation chemistry

2.1 Carbonation reactions

Alkaline wastes contain metal oxides, notably CaO and MgO, as well as other minerals such as brucite ($Mg(OH)_2$), serpentine ($Mg_3Si_2O_5(OH)_4$), forsterite (Mg_2SiO_4) and wollastonite ($CaSiO_3$) (Power et al., 2013). These minerals can be carbonated through either dry or aqueous methods. Although the dry carbonation of these minerals is spontaneous (e.g., for carbonation of serpentine and wollastonite, Liu et al. (2021) reported ΔG values of -16.9 kJ/mol, and - 44.6kJ/mol, respectively), it has a low rate, which can only be improved through different pre-processing steps. These pre-processing steps aim to release the MgO and CaO through energy-intensive processes before CO_2 uptake can take place (Zevenhoven and Kavaliauskaite, 2004). Consequently, dry carbonation is unlikely to be commercialised (Huijgen and Comans, 2005). Alternatively, aqueous carbonation has been reported to occur passively at different sites worldwide (Power et al., 2014). The first step in this method involves CO_2 dissolution and speciation according to the pH of the solution in which carbonation occurs. Archer (2007) explained that when water is in equilibrium with CO_2, the following system of reactions is established:

$$CO_2 + H_2O \rightarrow H_2CO_3 \leftrightarrow HCO_3^- + H^+ \quad (1)$$

$$HCO_3^- \leftrightarrow H^+ + CO_3^{2-} \quad (2)$$

The solubility of CO_2 in water depends on the CO_2 partial pressure and on the system temperature. In an aqueous solution, the speciation of CO_2 depends on the pH: at a low pH value, the equilibrium shifts towards H_2CO_3 to reduce the concentration of H^+, while under basic conditions, the equilibrium promotes more dissolution of H_2CO_3 to produce H^+ (Pan et al., 2012). This step can be limited due to poor mixing between the atmospheric CO_2 and the solution, slow transfer of CO_2 from

the gas phase to the liquid phase and slow CO_2 hydration (Power et al., 2013; Stumm and Morgan, 1996; Wilson et al., 2011).

The production of H^+ promotes silicate dissolution as shown in equation 3 in which M can be Ca or Mg (Daval et al., 2009):

$$M_xSi_yO_{x+2y-t}(OH)_{2t} + 2xH^+ \leftrightarrow \ xM^{2+} + ySiO_2 + (x+t)H_2O \quad (3)$$

Several studies have identified the dissolution of minerals to be the rate-limiting step in mineral carbonation (e.g., (Daval et al. (2009) and Pullin et al., (2019)). The dissolution of a mineral depends on the chemical structure of the mineral itself. Dissolution of minerals such as brucite proceeds faster than the dissolution of serpentine since brucite dissolution requires breaking a single type of bonds, while the dissolution of silicate-rich minerals requires breaking of several strong Si-O bonds (Power et al., 2013; Schott et al., 2009). Consequently, the dissolution of silicate-rich minerals may proceed non-stoichiometrically, leaving behind a silicon-rich passivating layer, as described by Schott et al. (2012), Power et al. (2013) and the references therein.

This dissolution reaction is then followed by precipitations reactions as shown in equations 4 and 5 (Daval et al., 2009):

$$xM^{2+} + \ xCO_3{}^{2-} \leftrightarrow \ xMCO_3 \quad (4)$$

Or

$$xM^{2+} + 2xHCO_3{}^- \leftrightarrow xMCO_3 + xCO_2 + xH_2O \quad (5)$$

2.2 Reaction parameters

Due to the huge variation in the chemical and physical properties of alkaline wastes, and due to the different reactions involved in mineral carbonation, optimizing CO_2 uptake requires finding the optimum conditions that enhance the steps of the carbonation reaction. For example, pH has variable effects on the carbonation

process. Lower pH increases metal leaching thereby increases the reactants' concentrations while higher pH promotes carbonates precipitation (Azdarpour et al., 2015; Chen et al., 2019). While increasing the temperature is associated with decreased CO_2 solubility in the aqueous solution (Huijgen et al., 2005), increasing the temperature from 10 ºC to 40 ºC was found to positively correlate with cations release from alkaline wastes, and the decreased solubility of CO_2 did not represent a limiting step (Assima et al., 2014a, 2014b). Increasing the CO_2 partial pressure has also been found to increase the carbonation as it enhances mineral dissolution and promotes carbonate mineral precipitation (Harrison et al., 2012; Pokrovsky and Schott, 2000). Additionally, climate conditions and atmospheric CO_2 concentration can affect the CO_2 uptake (Fig. 2). Due to the variations in carbonation mechanism and extent due to the chemical and physical variation of alkaline wastes, the quantification of the CO_2 uptake relies on combining information obtained from several analysis techniques, some of which are portrayed in Table 1.

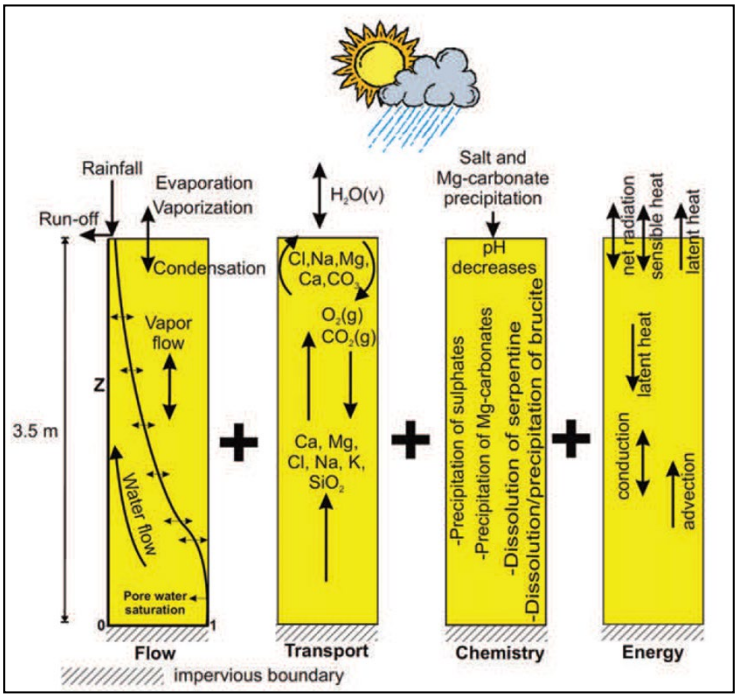

Fig. 2. Demonstration of interacting processes that affect CO_2 uptake in alkaline wastes in an arid environment. Reprinted from (Bea et al., 2012). Copyright (2012) with permission from Soil Science Society of America, Inc.

168 Table 1. Common analysis tools used in studying mineral carbonation of alkaline wastes

Method	Used for	Remarks	Reference
Thermogravimetric Analysis (TGA)	Study dehydroxylation of serpentine and minerals formation/recrystallization. Finding the weight fraction of $CaCO_3$ in a sample as it decomposes at a certain temperature range (500-1000 °C)	TGA cannot be used for quantification of different mineral phases within a sample. Thermal treatment of serpentine can increase the Mg released for carbonation. However, over heating should be avoided to avoid recrystallisation and production of less reactive minerals.	(Chiang and Pan, 2017; Dlugogorski and Balucan, 2014; Huijgen et al., 2005)
X-ray diffraction (XRD)	Qualitative/quantitative identification of mineral phases.	XRD can distinguish authigenic and pre-existing carbonates. Quantification of different phases in a semi-crystalline sample requires complicated methods such as Rietveld refinements.	(Wilson et al., 2009b, 2006)
Scanning electron microscopy (SEM)	Visualization of microstructures. Observing morphological changes upon carbonation. Identifying composition and mineral phases.	SEM imaging can be used to identify biological mineralisation of carbonates.	(McCutcheon et al., 2017; Ul-Hamid, 2018)
Total carbon/ organic carbon (TC/TOC)	Quantifying the amount of carbon within a sample	TOC/ TIC cannot distinguish between authigenic and pre-existing carbonates	(Dembicki, Jr., 2017; LECO Corporation, 2008)
X-ray computed tomography (XCT)	Observing the internal structures and morphology. Quantification and classification in 3D and 4D of mineral phases, porosity and pore connectivity, as well as individual grain analyses (shape, orientation, equivalent diameter, and so on).	XCT is suitable for studying in-situ carbonation. Geometry derived from XCT can be used as input for permeability modelling.	(Baker et al., 2012; Boone et al., 2014)
Stable isotope analysis	Quantify the origin of carbon in a sample (organic, lithogenic, atmospheric)	Stable isotope analysis can be corroborated with radiocarbon analysis to provide evidence of atmospheric CO_2 sequestration	(Renforth, 2011; Washbourne et al., 2012)

169

3. Studies of alkaline wastes carbonation

3.1 Iron and steel slag

The importance of steel in the global economy is evident from the production of over 3500 types of steel that are consumed in many industries, ranging from simple cooking equipment to spacecraft (Lai et al., 2012; World Steel Association, 2021). In 2017, it was estimated that for every 1000 kg of steel produced, around 1830 kg CO_2 is emitted, making this high emission the “biggest challenge” to this industry, as described by the World Steel Association (World Steel Association, 2019). The production of 1000 kg of steel results in around 200-400 kg slag, depending on the mode of production (World Steel Association, 2017). Recently, attempts have been made to utilize slag in sustainable cement and concrete manufacturing since using it as aggregate can decrease energy consumptions and emissions associated with concrete industries, without compromising the mechanical properties of products (Gencel et al., 2021). Experimentally, it was shown that the carbonation of slag can produce building materials with compressive strength that increase with increased CO_2 uptake (Wang et al., 2019).

As the United Kingdom (UK) has a rich history in iron and steel production, over 1.90×10^{11} kg of slag deposits exist in the country, providing excellent opportunities for studying passive carbonation within these alkaline wastes (Riley et al., 2020). Chukwuma et al. (2021) studied the weathering of iron and steel slag deposits in South Wales, UK which are associated with iron and steel production that ceased in 1980. These deposits contain calcium-silicate minerals, dominated by gehlenite ($Ca_2Al_2SiO_2$) and åkermanite ($Ca_2MgSi_2O_2$). Across the studied sites, the stored CO_2 in the slag was found to reach 66 kg CO_2 / 1000 kg slag. The carbon capture potential

194 can be estimated based on chemical compositions according to Steinour's formula
195 (Gunning et al., 2010; Renforth, 2019):

196 $$C_{pot} = \frac{MW_{CO_2}}{100}\left(\alpha\frac{CaO}{MW_{CaO}} + \beta\frac{MgO}{MW_{MgO}} + \gamma\frac{SO_3}{MW_{SO_3}} + \delta\frac{P_2O_5}{MW_{P_2O_5}}\right) \times 1000 \quad (6)$$

197 Where C_{pot} refers to the carbonation potential (kg CO_2 uptake/1000 kg wastes), CaO,
198 MgO, SO_3 and P_2O_5 refer to the percentages of the corresponding compounds, MW
199 refers to the molar mass, and the coefficients *α, β, γ, δ* consider the contribution of
200 different compounds and they are 1, 1, -1, -2, respectively (Chukwuma et al., 2021).
201 Consequently, the maximum measured CO_2 uptake was found to reach 77% of the
202 total carbonation potential.

203 Weathering of slag deposits at Consett, UK, provides another example of
204 passive CCS (Mayes et al., 2018). These 2 x 10^{10} kg deposits were produced over
205 100 years of operation (ended in 1980) of the Consett Iron and Steel Works that
206 produced around 1.2 x 10^{11} kg of iron and steel (Mayes et al., 2018). XRD analysis
207 revealed that the slag was dominated by melilite minerals, and that the downstream
208 precipitate is almost entirely composed of calcite (Mayes et al., 2018; Pullin et al.,
209 2019). By referring to slag density and chemical compositions, the largest heap was
210 estimated to have the potential to sequester 6 x 10^9 -1.1 x 10^{10} kg CO_2 through mineral
211 carbonation (Mayes et al., 2018). However, based on the draining water chemistry and
212 calcium leaching and calcite precipitation rates, between 2.81 x 10^5 and 2.89 x 10^6 kg
213 CO_2 has been sequestered since 1980, due to the limited inflow of CO_2 into the heap
214 and due to the surface passivation of slag with carbonate (Mayes et al., 2018). This
215 site was further studied by Pullin et al. (2019) after *Geosonic Drilling Company* drilled
216 three boreholes across a 60 m transact. CO_2 concentrations in the boreholes were
217 almost 85 ppm, while they reached almost 403 ppm at the surface, reflecting that the
218 produced slag has had little interaction with the atmospheric CO_2 (Pullin et al., 2019).

With total carbon concentration of 0.42%, Pullin et al. (2019) estimated that only ~ 3% of CO_2 capture potential was utilized.

The production of 1000 kg of steel generates 400 kg of slag and emits 1830 kg of CO_2 (World Steel Association, 2019, 2017), The previous studies demonstrate that CO_2 can be passively sequestered within slag. The maximum theoretical CO_2 uptake in slag is controlled by slag composition and is dictated by CaO and MgO content (Mayes et al., 2018). With CaO and MgO concentrations vary from 29% to 44% and 5% to 12% respectively (Proctor et al., 2000), it is possible to calculate that utilizing slag can sequester 113-190 kg CO_2, or ~10% of CO_2 emitted from the production of 1000 kg of steel, based on the complete conversion of CaO and MgO. However, as depicted earlier, the CO_2 uptake is much less than the maximum theoretical CO_2 uptake due to several factors. Ca and Mg are usually incorporated into more complex mineral structures (Yildirim and Prezzi, 2015). Several slag-forming minerals have been identified in the literature, and these minerals have variable carbonation rates (Bodor et al., 2013). These minerals are produced during slag cooling and their presence is affected by the waste management practice. For example, the cooling rate has been determined to result in different mineral compositions in slag (Kriskova et al., 2013). Rapid cooling produces more reactive slag composed of tricalcium silicates while slow cooling produces åkermanite or gehlenite phases that are less reactive (Engström et al., 2013; Pullin et al., 2019; Scott et al., 1986). Another issue that reduces the CO_2 uptake in slag is that slag may be produced at gravel size causing it to have a low surface area thereby lowering its CO_2 uptake rate (Ragipani et al., 2021).

3.2 Demolition wastes in artificial soil

Artificial soils in urban and brownfield land originate from demolition and construction wastes and provide an opportunity for CCS as they are rich in Ca- and

Mg-silicates. These compounds can interact with carbon which originates from the dissolution of CO_2 from plant respiration and decomposition, or from CO_2 dissolving in alkaline water, to produce carbonates (Renforth, 2011). This section reviews studies that investigate the applicability of artificial soils and demolition wastes in CCS applications.

Jorat et al. (2020) investigated soil carbonation in over 20 brownfield sites across the UK by calculating soil carbonation rates and observing carbonation effects on permeability and ground strength. Carbonation rate was measured through TIC measurement of soil to a depth of 20 cm and presented as a function of site age, where the latter was defined as the period between the demolition and the sampling dates. Throughout the study period, sites aged between 7 and 26 years had no significant change in TIC, while there was a statistically significant increase in TIC for three young sites aged between 2 and 8 years (Jorat et al., 2020). Carbon sequestration occurred at a rate of 100-1600 g C m^{-2} y^{-1}, indicating that the higher carbonation rate occurred at more modern sites as they were more suitable for carbonation, possibly due to their inclusion of more fine-grained crushed concrete (Jorat et al., 2020).

The Science Central Park in Newcastle, UK, has been the subject of passive carbonation studies (Washbourne et al., 2012, 2015). The 10^5 m^2 site is made up of a 0.2-6 m thick layer of made ground, which contains crushed concrete and aggregate. Washbourne et al. (2015) studied soil carbonation at this site for 18 months. Over the study period, the $CaCO_3$ content within the top 100 mm of the soil increased from 5.3-43 wt % $CaCO_3$ to 26.5-61.4 wt% $CaCO_3$, where the ranges reflect the content at different locations within the study site (Washbourne et al., 2015). $CaCO_3$ content did not vary with depth in a consistent manner, although it was observed that for some pits the concentration was larger at shallow depths of less than 1 m, and a decline was

observed when the depth exceeded one meter (Washbourne et al., 2015). During the 18-month study period, CO_2 was sequestered at a rate of 2320 g C m^{-2} y^{-1} with calcite being the dominant phase of $CaCO_3$ (Washbourne et al., 2015).

Based on the estimations of Renforth et al. (2009) and the references therein, brownfields occupy 1.45 x 10^{10} m^2 globally. With a measured CO_2 uptake of 30 ± 15.3 kg C m^{-2}, it can be estimated that brownfields have already captured 4.353 x 10^{11} kg C (Renforth et al., 2009). The annual concrete wastes production reaches 6.8 x 10^{12} kg y^{-1}, and it has a maximum carbon capture potential of 2.9 x 10^{11} kg C y^{-1}, assuming it contains 20% CaO (Renforth et al., 2009). However, achieving high CO_2 uptake in demolition wastes is usually challenged by several factors. After the service life of a structure, it is destructed to produce concrete ruble which is then crushed and stockpiled for a period between 2 weeks and 4 months (Pade and Guimaraes, 2007). Importantly, the size of demolition waste materials is a critical factor in their CO_2 uptake, with sizes larger than 40 mm were found to be unsuitable for carbonation (Butera et al., 2015). While CO_2 uptake in concrete aggregate increases after demolition as a result of pulverization, it is also affected by the end use of the pulverized concrete. Crushed concrete in most countries is used in the manufacturing of roads and other below-ground applications, thereby reducing its CO_2 uptake (Marinković et al., 2014; Pade and Guimaraes, 2007).

3.3 Mine tailings

Modern industry consumes high quantities of metals, making mining operations pivotal in economic development. According to the Mining, Minerals and Sustainable Development (MMSD) Project, there are more than 3500 active mining waste facilities globally (Tayebi-Khorami et al., 2019), resulting in producing mine wastes at a rate of 2 x 10^{12} - 6.5 x 10^{12} kg y^{-1} (Renforth et al., 2011), and Power et al. (2013) estimated

that around 4.19 x 10^{11} kg of mafic and ultramafic wastes are produced annually. Mineral compositions of tailings allow them to sequester CO_2 and offset emissions from mining industries. The carbonation capacity of tailings is associated with the complete conversion of their Ca and Mg to carbonates on a mole per mole basis (Paulo et al., 2021). Several minerals, such as brucite, lizardite, diopside, forsterite and wollastonite have been identified as possible sources for cations although these minerals have different dissolution rates. Brucite has the highest dissolution rate across a wide range of pH values that is orders of magnitude larger than that of Mg-silicate minerals (Power et al., 2013). Nevertheless, other silicate minerals such as serpentine provide significant CO_2 uptake capacity as they release magnesium that is loosely bound to the silicate surface (Assima et al., 2013; Stubbs et al., 2022; Vanderzee et al., 2019).

3.3.1 Nickel mining

Passive carbonation of mine tailings and waste rocks associated with nickel mining operations in Québec, Canada has been the subject of some studies (Gras et al., 2020, 2017, 2015). The CO_2 uptake by these wastes was estimated by following the carbonation over a 4-year period using two different setups: the first one, referred to as EC-1 cell, contained 1.04 x 10^5 kg of heterogeneous waste rocks, ranging from block to silt size, and a second cell, referred to EC-2 cell, contained ~2.1 m^3 of mine tailings (Gras et al., 2017). The dominant mineral phases were chrysotile, lizardite, brucite and magnetite, while minor amounts of calcite and millerite were present (Gras et al., 2017; Pronost et al., 2010). Upon weathering, crusts formed on the surface of most rock fragments in EC-1 and near the edges of the tailings in EC-2 (Gras et al., 2017). In both cells, the CO_2 concentration decreased from the atmospheric value of 390 ppmv at the surface, to 50 ppmv and 25 ppmv in EC-1 and EC-2, respectively,

and the CO_2 drop increased as the depth increased. CO_2 concentration within both cells increased from year to year and this increase was accompanied by a reduction of brucite peak in the XRD analysis and an increase in carbonate minerals. Therefore, the reduction of the carbon capture rate was attributed to the consumption of the brucite or the surface passivation due to the formation of carbonate (Gras et al., 2017).

Wastes from nickel mining were also investigated to quantify the carbonation process in Mount Keith, Western Australia (Wilson et al., 2014). XRD analysis of several samples collected from the tailing facilities showed that the majority of minerals were serpentines, including antigorite and lizardite, and hydrotalcite minerals, including iowate and woodalite. There were also minor amounts of brucite, chrysotile, calcite and dolomite. Efflorescence was spotted at the surface of the tailings, and it was dominated by hydromagnesite, halite and hexahydrate. Hydromagnesite was also detected in most of the collected samples, and its highest presence was recorded at shallow depths, mostly filling cracks and fissures of serpentine or on the surface of serpentine grains. The abundance of brucite/serpentine decreased with time, while the amount of hydromagnesite increased (Wilson et al., 2014). The greatest amount of hydromagnesite was recorded in the top 25 cm of the tailings, coinciding with the lowest amount of serpentine and brucite. Current rates of passive carbon mineralization offset ~11% of greenhouse gases emitted from Mount Keith mine, and enhancing carbon mineralization to carbonate the brucite alone will result in offsetting the CO_2 emissions from Mount Keith mining by at least 20% (Harrison et al., 2012; Wilson et al., 2014).

3.3.2 Chrysotile mining

Due to the health problems of asbestos, chrysotile mining has significantly decreased (World Health Organization, 2014). However, there are several chrysotile

tailings sites that provide excellent opportunities to study and quantify mineral carbonation within chrysotile tailings. For example, Clinton creek in Yukon Territory, Canada hosts $1x10^{10}$ kg of tailings (Indian and Northern Affairs Canada, 2008; Wilson et al., 2009a). Nesquehonite was observed to form towards the surface of the tailings as a result of evaporative precipitation, while dypingite and hydromagnesite were observed to cement serpentine grains below the nesquehonite-covered surfaces, or on the surface of cobbles. High CO_2 uptake of 1.64×10^8 kg was calculated, corresponding to 6.3×10^6 kg CO_2 y^{-1} when considering the age of 26 years (Wilson et al., 2009a, 2006).

Oskierski et al. (2013) investigated the carbonation potential of chrysotile mine tailings within Woodsreef asbestos mine in Australia, where mining took place between 1906 and 1983, producing about 5.5×10^8 kg of fibers from 2.5×10^{10} kg ore, most of which was produced between 1971 and 1983 (Brown et al., 1992; Oskierski et al., 2013). At the studied location, there were several modes of carbonate occurrence, including horizontal and vertical crusts. Crust samples were analyzed through XRD analysis which revealed the predominance of serpentine minerals (Oskierski et al., 2013). Brucite and carbonate minerals, such as hydromagnesite, pyroaurite, calcite, dolomite and magnesite, were present at varying amounts. Around 1.4×10^6 kg of CO_2 are stored within the crusts, providing a lower estimate of the carbonation (Oskierski et al., 2013). An upper estimate of 7.0×10^7 kg CO_2 can be calculated if pyroaurite, which was estimated to have a concentration of 4.3 wt% within the tailings pile, is also considered as product of mineral carbonation. Considering that carbonation has occurred since the closure of the mine over a period of 29 years, the carbonation rate was calculated to be between 27 g C m^{-2} y^{-1} and 1330 g C m^{-2} y^{-1} (Oskierski et al., 2013). Oskierski et al. (2016) highlighted the importance of

evaporation in carbonate precipitation, as evident from the high δ ^{18}O signature in the precipitated hydromagnesite, and the high values of $\delta^{13}C$ that was associated with evaporative enrichment prior to precipitation (Oskierski et al., 2021, 2016).

Woodsreef mine wastes were further studied in later research which investigated the mineral composition of the top 120 cm of the mine wastes (Turvey et al., 2018b). The amount of captured CO_2 was estimated using two different approaches: i) quantitative XRD, where the mineral composition was estimated using structureless fitting methods, as explained elsewhere (Turvey et al., 2018b, 2018a, 2017) and the references therein; ii) and by measuring the total elemental carbon and then finding the inorganic carbon by assuming an average value of the organic carbon to be 0.02 wt % C as suggested in the literature (Hamilton et al., n.d.; Turvey et al., 2018b). XRD data demonstrated that the presence of several forms of carbonates varied with depth. To provide conservative estimates of carbonation rates, it was assumed that carbon sequestration occurred within the top 120 cm of the tailing. XRD analysis showed that there were different modes of carbonation occurring within the study region: in the shallow depths (up to 40 cm), CO_2 sequestration occurred as a result of brucite carbonation that produces hydromagnesite. On the other hand, at larger depth where CO_2 supply is limited, coalingite and pyroaurite were the primary carbonation products, as portrayed in Fig. 3. The carbon content based on XRD data and elemental carbon measurement through the studied region was found to be 3.9 x 10^6 kg CO_2 and 6.9 x 10^6 kg CO_2, respectively. The value obtained from the XRD provides a lower estimate, since XRD analysis does not take into account the carbon that resides in amorphous structures, and the quantification method was shown to underestimate the amount of carbonates within tailings (Turvey et al., 2018a). On the other hand, as the elemental carbon data report the total carbon content, without

restricting the amount of carbon to the minerals that were produced as a result of CO_2 sequestration, the obtained value reflected the upper estimates of the CO_2 sequestration at Woodsreef. Considering these end members, the carbonation potential was estimated to be between 62 and 110 g C m^{-2} y^{-1}, a range that overlaps with the carbonation range reported by Oskierski et al. (2013). Turvey et al. (2018b) attributed this to the fact that Oskierski et al. (2013) estimated that pyroaurite has a concentration of 4.3%, which was proven to be not the case, as shown in Fig. 3. More representative values of CO_2 sequestration can be obtained by obtaining mineralogical composition and carbon content at higher depth within tailings.

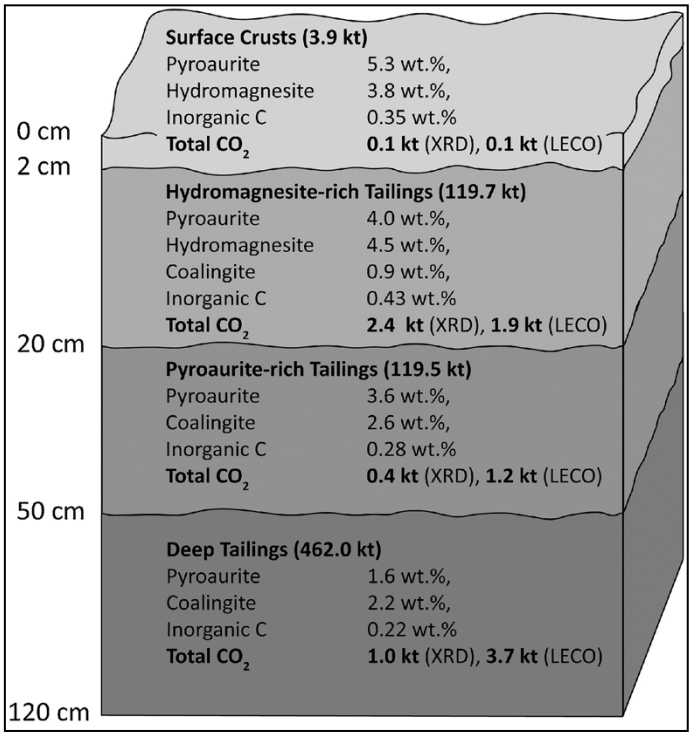

Fig. 3. Variation in mineralogical composition and CO_2 sequestration with depth at Woodsreef mine tailings. Values next to XRD represent the amount of CO_2 sequestered as estimated using XRD analysis while values next to LECO represent the amount of CO_2 sequestered as estimated using total elemental carbon. Reprinted from (Turvey et al., 2018b), Copyright (2018) with permission from Elsevier.

3.3.3 Kimberlite mining

Kimberlites are volatile-rich, ultramafic rocks that are being mined for diamonds. (Mitchel, 1986; Wilson et al., 2011). There is some evidence that processed kimberlite

412 can sequester atmospheric CO_2. For example, it was estimated that around 1.8 x 10^6
413 kg CO_2 may have been sequestered in the processed kimberlite at the Diavik diamond
414 mine in the Canadian northwestern territories (Wilson et al., 2009b). At Diavik, the
415 processed kimberlite contained serpentine minerals, forsterite and minor amounts of
416 other minerals, including clay minerals, Mg-rich garnet and plagioclase feldspar
417 (Wilson et al., 2011, 2009b). Nesquehonite was the most common form of secondary
418 carbonates, taking the shape of continuous films at the surface of the tailings. Wilson
419 et al. (2011) reported that nesquehonite formed on the surface of forsterite and
420 serpentine, indicating that it precipitated due to mineral weathering, resulting in
421 trapping of carbon at a rate of 102-114 g C m^{-2} y^{-1}, which is two orders of magnitude
422 higher than natural silicate weathering in river catchments in areas with similar climatic
423 conditions (Huh, 2003; Wilson et al., 2011). The waste management practice, in which
424 the tailings are stored under process water, severely limits the carbonation rate
425 (Wilson et al., 2011, 2009b).

426 Mervine et al. (2018) studied the carbonation potential of processed kimberlite
427 in different mines in Canada and in South Africa. Several minerals with high
428 carbonation potentials were detected, including serpentine, olivine, brucite, and
429 smectite. Serpentine was the most abundant mineral, having the bulk of CO_2 capture
430 potential associated with its high content of labile Mg^{2+} (Mervine et al., 2018; Stubbs
431 et al., 2022; Vanderzee et al., 2019). Although present at a small fraction, brucite is
432 important as it can be carbonated at relatively low temperature and pressure. Different
433 forms of carbonates, including calcite, dolomite, magnesite and siderite were detected
434 at variable concentrations. Using the mineral and chemical properties of the kimberlite
435 and carbonation potential correlation published elsewhere (Wilson et al., 2009b), it
436 was estimated that carbonation of 4.7 to 24 wt% of the annual processed kimberlite

437 can result in offsetting 100% of CO_2 equivalent emitted from each mining site (Mervine
438 et al., 2018).

439 **3.3.4 Red mud**

440 Red mud is produced from bauxite/aluminum ore processing. Due to its
441 physical and chemical properties, notably ductility and malleability, aluminum is the
442 most used metal after iron and steel (Geoscience Australia, 2018). Red mud is
443 produced at a rate of 1-1.5 kg per kg of produced alumina (Al_2O_3) (Yang and Xiao,
444 2008), resulting in a world stock of ~4 x 10^{12} kg in 2015 (Gore, 2015; Mukiza et al.,
445 2019). Most of today's alumina is produced through the Bayer process, which involves
446 mixing the finely ground ore with caustic soda (Geoscience Australia, 2018). The
447 produced alumina is in turn smelted through the Hall-Héroult smelting process to
448 produce aluminum (Geoscience Australia, 2018). The by-product residue is thickened
449 in a process known as dry stacking. Mixing the residue with CO_2 can reduce the pH of
450 the suspension from 13 to less than 10.5, making the slurry more suitable for biological
451 activities that promote the breakdown down of organic residues. Residue carbonation
452 has been found to enhance drying rates, requiring less area thereby resulting in
453 aesthetic and cost benefits (Alcoa, 2012).

454 Red mud has a potential to passively sequester CO_2 at ambient conditions. Si
455 et al. (2013) investigated the carbonation potential of different red mud residues that
456 were collected from different aluminum refineries in China and Australia. They
457 calculated the maximum carbonation potential (which they defined as the total
458 alkalinity of red mud, assuming that 2 moles of OH^- can capture 1 mole of CO_2) and
459 actual carbonation (defined as total carbon concentration of red mud) and revealed
460 that the maximum carbonation significantly exceeds the actual carbonation by up to
461 more than 100%. This was attributed to the treatment of red mud with seawater, which

462 removes a considerable amount of alkali metals that could have been utilized in
463 carbonation. Additionally, XRD analysis detected perovskite and larnite, indicating that
464 TiO_3^{2-} and SiO_4^{2-} compete with carbonate for Ca^{2+}. Based on the current red mud
465 production rate of 1.2 x 10^{11} kg y^{-1} (Power et al., 2011) and based on the estimated
466 CO_2 uptake of 15 kg C / 1000 kg red mud, Si et al. (2013) estimated that approximately
467 6x10^9 kg of CO_2 can be sequestered within red mud annually, and another 6x10^9 kg
468 CO_2 can be sequestered if adequate technologies (such as supplying of Ca^{2+}) are
469 used.

470 Renforth et al. (2012) investigated the accidental release of a high quantity (6 x
471 10^5 – 7 x 10^5 m^3) of hyper alkaline (pH= 13) red mud in Ajka, western Hungary (Urbán
472 and Cséplı, 2010). Atmospheric CO_2 readily ingresses in such hyperalkaline solutions.
473 As a mitigation strategy, gypsum was added since it provides a source of Ca^{2+} and
474 result in precipitation of calcium carbonate resulting in decreasing the pH, as show in
475 equation 7:

476 $$2\,OH^- + CaSO_4 \cdot 2H_2O + 2CO_2 \leftrightarrow CaCO_3 + {SO_4}^{2-} + 2H_2O + H_2CO_3 \quad (7)$$

477 Based on carbonate, elements, and stable isotope analysis, it was shown that
478 high sulfur content was strongly correlated with high atmospheric CO_2 sequestration.
479 It was calculated that mixing 1000 kg of red mud with 860 kg of gypsum can result in
480 sequestration of 220 kg CO_2. With the figures of gypsum and red mud production rates
481 that are reported in Renforth et al. (2012) and the references therein, it was estimated
482 that red mud carbonation through gypsum addition can sequester around 1.3 x 10^{10} -
483 2.6x10^{10} kg CO_2 which corresponds to 3 - 4% of CO_2 emitted from primary production
484 of aluminum (Harnisch et al., 1998; Renforth et al., 2012).

485 The idea of adding Ca^{2+} sources to neutralize alkaline red mud was also
486 investigated by Han et al. (2017). Particularly, the effect of adding gypsum or calcium

chloride on enhancing the sequestration potential of bauxite residue and on the pH reduction was studied on two scales: 55-day batch tests, during which the pH values of slurry solutions were reduced using atmospheric CO_2 at ambient conditions, and field neutralization tests, during which 100 kg of bauxite was distributed over a 4 m^2 area for 120 days. Batch tests demonstrated that carbonation decreased pH to 9.5 (bauxite residue), indicating consumption of pore water alkalinity. The addition of Ca^{2+} sources decreased the pH further, as demonstrated for the gypsum-treated and $CaCl_2$-treated residues, for which the pH dropped to 8.3 and 7.7, respectively. Han et al. (2017) quantified that it is possible to sequester 0.083 g CO_2 to neutralize 1 g of bauxite residue, or to $2.3x10^7$ kg CO_2 per the $2.8x10^8$ kg of bauxite residue produced in Korea.

Another study (Khaitan et al., 2010) investigated simultaneous CO_2 sequestration and bauxite residue neutralization at two different locations in Texas, US, namely the Sherwin and Copano bauxite storage facilities, aged 35 and 14 years at the time of study, respectively. The older site had lower pH; the surface pH at Sherwin was 9.5, while at Copano it was 10.5. Total carbon was higher at Sherwin and in both sites, and there was a trend showing that higher carbonation extent occurred closer to the surface. Moreover, XRD results at Copano showed that a more pronounced peak of calcite occurred at the surface accompanied by a decrease in tricalcium aluminate as compared to deeper regions. Atmospheric CO_2 could reduce the pH of red mud, and the existence of some vegetation such as bitter weed and Bermuda grass could further reduce the pH to 9, in alignment with increased carbon content in vegetated locations.

3.4 Summary: alkaline wastes carbonation potential

Annually, around 7 x 10^{12} kg of silicate wastes are produced on the global scale (Renforth et al., 2011). Using Steinour's formula (equation 6), Renforth (2019) estimated the carbon capture potential of these wastes, as shown in Fig. 4. Renforth (2019) modelled the production of alkaline wastes and their contributions to carbon mitigation strategies based on different socioeconomic pathways, which are scenarios that enable an analysis of future climate impacts, vulnerabilities, mitigation and adaptation based on several drivers, such as urbanization, population and economic growth (Riahi et al., 2017). CO_2 emissions are predicted to be between 2.4 x 10^{13} - 1.26 x 10^{14} kg CO_2 y^{-1} by 2100, and CO_2 uptake potential within alkaline wastes can be between 2.9 x 10^{12} - 5.9 x 10^{12} kg CO_2 y^{-1}. In other words, alkaline wastes can mitigate 5-12 % of CO_2 emissions (Renforth, 2019).

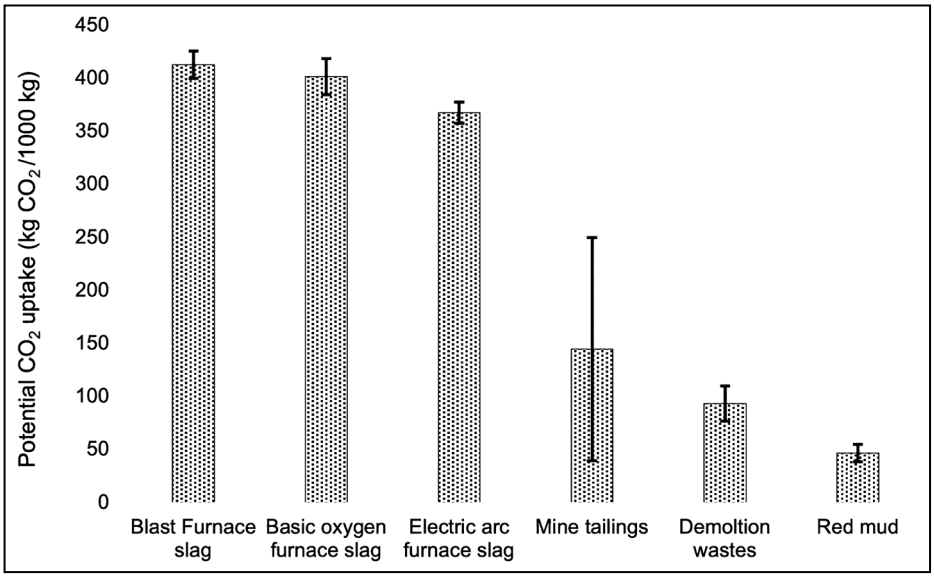

Fig. 4. CO_2 capture potential of various alkaline wastes. Error bars reflect variation of carbonation potentials as a result of different compositions. The figure is based on data from (Renforth, 2019)

Clearly, the studied wastes can offset significant amounts of CO_2 emissions. Nevertheless, the CO_2 uptake potential of alkaline wastes can be overestimated. This is because it is calculated based on the conversion of Mg and Ca to carbonate minerals on a mole per mole basis. Paulo et al. (2021) explained that the source of

these cations should be considered in the estimation of carbonation capacity, since these cations may be present in carbonate minerals, and carbonates are an undesirable source of cations. Consequently, Paulo et al. (2021) suggested a leaching test that is coupled with a TIC test to identify the cations that reside in carbonates and to exclude them from carbonation capacity calculations.

Table 2 reports the CO_2 uptake at various locations showing. At Mount Keith, passive sequestration offsets 11% of annual emissions and has carbon capture potential that exceeds the emissions by a factor of 10 (Wilson et al., 2014). A smaller offset is observed at Diavik in Canada where the tailings offset 0.2% of the emissions due to the arid and cold climate in that region and due subaqueous waste storage (Wilson et al., 2011). Though it is difficult to compare carbonation rates since minerals, emplacement and climate conditions vary, Table 2 shows that carbonation rates from reviewed sites are generally in the same order of magnitude, and carbonation occurs even in subarctic and arid climates. One issue to be addressed is that the reported CO_2 uptake values are based on different assumptions. For example, the value provided for Clinton creek was based on two samples: the first sample was assumed to be representative of 2/3 of the tailings while the second one was assumed to be representative of 1/3, and the overall CO_2 uptake was estimated based on the composition of these sample (Wilson et al., 2006). On the other hand, Turvey et al. (2018b) reported the distribution of the minerals with depth and considered the incomplete conversion to hydrotalcite minerals in the estimation of carbonation. Clearly, different methods may result in different estimation of CO_2 uptake in alkaline wastes.

552 Table 2. CO_2 uptake and the observed carbonates at different sites

Commodity	Location	CO_2 uptake	Observed carbonates	Remarks	Reference
Slag	Consett, UK	$7.6x10^3$-$7.8x10^4$ (kg CO_2/y)	Calcite	$\delta^{13}C$, $\delta^{16}O$ data suggest that between 54% and 99% of the precipitated carbon is from atmospheric origin and the rest is from lithogenic origins.	(Mayes et al., 2018)
Slag	Ohio, United states	0.23 – 3.94 (kg CO_2 /1000 kg slag / y)	Calcite	The slag was used to neutralize acid-mine drainage, and the provided uptake value is based on PHREEQC calculations.	(Goetz and Riefler, 2015)
Demolition wastes	Several towns in England, UK	0.4–5.9 (kg CO_2/m^2/y)	Calcite	The largest amount of CO_2 was captured during the first 15 years after demolition. $\delta^{13}C$ and $\delta^{16}O$ suggest the removal of CO_2 from the atmosphere via biological and chemical processes.	(Jorat et al., 2020)
Nickel wastes	Dumont, Québec, Canada	0.60-2.2 (kg CO_2/m^2/y)	Hydrotalcites, aragonite, nesquehonite, dypingite and hydromagnesite	$\delta^{13}C$ and $\delta^{16}O$ suggest precipitation of carbonates under an evaporative environment.	(Gras et al., 2017; Kandji et al., 2017)
Chrysotile wastes	Woodsreef, Australia	0.099- 4.9 (kg CO_2/m^2/y)	Hydromagnesite, hydrotalcite, dolomite, calcite, magnesite	High values of $\delta^{13}C$, $\delta^{16}O$ and F14C in hydromagnesite suggest precipitation form atmospheric CO_2 contained in meteoric water. For pyroaurite, the $\delta^{13}C$, $\delta^{16}O$ are close to those of bedrock, although it contained significant radiocarbon.	(Oskierski et al., 2013)
Chrysotile wastes	Woodsreef, Australia	0.229-0.405 (kg CO_2/m^2/y)	Hydromagnesite, coalingite and pyroaurite	Availability of CO_2 affect the type of carbonate produced. At a shallow depth, hydromagnesite is produced while at a larger depth, hydrotalcite is produced. Modern atmosphere CO_2 was found to be a source of carbon in the precipitated hydromagnesite and pyroaurite.	(Turvey et al., 2018b)
Chrysotile wastes	Yukon, Clinton creek, Canada	6.2 (kg $CO_2/m^2/y^1$)	Nesquehonite hydromagnesite, dypingite, lansfordite	Several modes of carbonates were observed, including cements, cobble coatings and crusts. Values of $\delta^{13}C$, $\delta^{16}O$ and $F^{14}C$ indicate carbonates formation from modern CO_2.	(Schuiling et al., 2011; Wilson et al., 2009a)

Chrysotile wastes	Thetford, Québec, Canada	0.98 - 120 (kg $CO_2/m^2/y$)	Hydromagnesite, pyroaurite, sjögrenite	The exothermic CO_2 mineralization reaction resulted in warming the air that vent the surface of chrysotile heap. This warm air is CO_2 depleted, in winter, this air contained 10-18 ppm CO_2, while in summer it contained 260-370 ppm CO_2	(Lechat et al., 2016; Pronost et al., 2012)
Kimberlite wastes	Diavik NT, Canada	0.374-0.418 (kg $CO_2/m^2/y$)	Nesquehonite, dolomite, calcite, vaterite, and other Na/Ca bearing carbonates	$\delta^{13}C$, $\delta^{16}O$ and F14C analyses suggested that at least 89% of carbon in secondary carbonates is sourced from the atmosphere either directly or through biological activity.	(Wilson et al., 2011)

553

554 # 4. Limitations of passive carbonation

555 ## 4.1 Slow carbonation due to limited CO2 supply

556 One of the primary reasons for the low carbonation rate of alkaline wastes is
557 the low concentration of CO_2 in the atmosphere. Passive carbonation relies on using
558 atmospheric air which is ~0.04% CO_2, causing it to be more difficult when compared
559 to techniques that use a concentrated CO_2 stream (Buis, 2019; Wilcox et al., 2017).
560 Therefore, increasing the exposure of wastes to CO_2 has been suggested as a method
561 to increase CO_2 uptake. In a study that investigated the carbonation of a subarctic
562 chromite mine shaft in Norway, it was noted that air circulation can enhance the
563 carbonation (Beinlich and Austrheim, 2012). For mines that have a single entrance,
564 carbonation was limited near the entry point while for mines that have multiple
565 entrances, air circulation was enhanced and carbonation was observed to occur
566 throughout these mines. Harrison et al. (2012) studied the carbonation of brucite, at
567 conditions that mimic those at Mount Keith nickel mine. They investigated the effect of
568 increasing the CO_2 concentration, under a system pressure of 0.1 MPa, on the
569 carbonation of brucite, and demonstrated that as the concentration of CO_2 increased
570 from 0.04% to 100%, the carbonation rate increased by ~2400 fold. This carbonation
571 rate can offset up to ~57% of CO_2 emissions from Mount Keith nickel mine (Harrison
572 et al., 2012).

573 Different carbonation products may form in different environments, depending
574 on CO_2 availability. In environments where CO_2 supply is limited, incomplete
575 carbonation can produce hydrotalcite minerals. This was documented at Woodsreef
576 where at shallow depth hydromagnesite ($Mg_5(CO_3)_4(OH)_2{\cdot}4H2O$) is produced while
577 hydrotalcite minerals such as pyroaurite ($Mg_6Fe_2^{3+}(CO_3)(OH)_{16}{\cdot}4H2O$) and coalingite

578 ($Mg_{10}Fe_2^{3+}(CO_3)(OH)_{24}\cdot 2H_2O$) are produced at larger depths where CO_2 supply is
579 limited (Turvey et al., 2018b). The work of Turvey et al. (2018b) provides evidence that
580 increasing CO_2 availability in tailings results in the formation of more efficient CO_2
581 sinks that can sequester a higher amount of CO_2 for a given amount of Mg and result
582 in a lower volume of precipitated carbonates.

583 ## 4.2 Carbonation reduction due to negative feedbacks

584 Negative feedback loops can be caused by the carbonation reaction products
585 which precipitate at or near the reactive sites and thus prevent CO_2 from reaching
586 those sites. This behaviour has been reported particularly in ex-situ carbonation
587 studies. For example, Chang et al. (2012) observed that as pulverized slag (<63 μm)
588 is carbonated, a layer of carbonate forms around the particle, and its thickness
589 increases as the reaction proceeds, resulting in limiting further carbonation. The
590 generation of the passivation layer can also result from silanol polymerization. Assima
591 et al. (2013) investigated this issue by studying CO_2 uptake in chrysotile mining wastes
592 that contained different amounts of water. For a given amount of water, Assima et al.
593 (2013) showed that increasing the watering frequency positively correlated with
594 increasing CO_2 uptake. Higher watering frequency resulted in Mg^{2+} supersaturation
595 in pore water and increased its pH, resulting in more carbonate precipitation. When
596 water was added, it transported the carbonation products to larger depths and allowed
597 upper pores to host further carbonation reactions. Additionally, it was demonstrated
598 that the addition of water on episodes reduces surface passivation through silica gel
599 polymerisation, since polymerisation is promoted when an excess amount of water is
600 added (Assima et al., 2012; Grénman et al., 2008). It should be noted that carbonation
601 may be reduced as a result of permeability reduction caused by carbonates
602 precipitation. However, Assima et al. (2013) observed that when chrysotile wastes

603 interact with CO_2-lean stream in a saturation-controlled porous bed, the pressure drop
604 decreased as the carbonation progressed, reflecting that clogging was outpaced by
605 dissolution.

606 However, it should be noted that volume expansion can cause a positive
607 feedback, which is explained by a “reaction driven cracking” as explained by Kelemen
608 et al. (2020) and the references therein. In this process, volume expansion due to the
609 carbonation causes differential stresses which in turn cause fractures that enhance
610 the permeability and facilitate delivery of reactants to reactive sites, thereby enhancing
611 the degree of carbonation as observed in carbonates precipitation in mines walls and
612 ceilings (Beinlich and Austrheim, 2012). Understanding the chemo-mechanical factors
613 can help in establishing a phase diagram that elucidates the conditions that promote
614 positive feedback and carbonation enhancement (Kelemen et al., 2020).

615 4.3 Waste generation and management practice

616 Alkaline wastes have the potential to sequester 1.90×10^{11} - 3.32×10^{11} kg C y^{-1}
617 (Renforth et al., 2011). Yet this potential is hindered because when tailing storage
618 facilities were designed, mineral carbonation had not been considered. Waste
619 management practice can be tailored to favour CCS by enhancing cations leaching
620 (Power et al., 2014). This can be done through different pathways, for example, by
621 acidity generation through bioleaching using different kinds of bacteria, such as *L.*
622 *ferrooxidans*, *A. ferrooxidans* and *A. thiooxidans* (Edwards and Goebel, 1999;
623 Nordstrom and Southam, 1997; Power et al., 2014). These bacteria decrease the pH
624 by producing sulfuric acid through bio-oxidation of sulphur that exists within minerals
625 in copper, uranium and gold ores. Power et al. (2010) reported that the addition of
626 sulphur (which acts as an acid-generating species) and *A. thiooxidans* to tailings
627 increased the concentration of magnesium in leachates by an order of magnitude. This

magnesium-rich leachate can be transferred to carbonation ponds where cyanobacteria is added to generate alkalinity and to provide nucleation sites for carbonate precipitation (McCutcheon et al., 2016; Power et al., 2010).

Additionally, passive carbonation can be enhanced by increasing the contact between tailings and the atmosphere and/or water, whether from meteoric or process sources (Power et al., 2014). For a given deposition rate, increasing the number of deposition points results in decreasing the period during which tailing are deposited over a given area, allowing for a formation of thinner tailings that cover a larger area (Wilson et al., 2014). At Mount Keith mine, tailings are deposited from nine risers that are concentrated towards the center of the tailings storage facility. Increasing the number of risers results in a more thin and uniform distribution of tailings across a large surface area, allowing for more time for mineral carbonation and CO_2 sequestration, as was shown through reactive transport modelling done by Wilson et al. (2014) (Fig. 5). Alternatively, using forced-air systems to enhance air circulation inside wastes piles has also been suggested, based on numerical modeling that showed that CO_2 concentration is reduced inside the waste piles since the mineralization rate is higher than the CO_2 supply rate (Nowamooz et al., 2018). Power et al. (2014) established a decision tree for choosing a waste management practice, based on the availability of resources (water, waste organics, and area) and sources of CO_2, whether from the atmosphere or a concentrated CO_2 stream, as depicted in Fig. 6. In Scenario A, low carbon can be enhanced by introducing waste organics or by increasing the waste deposition area, making this scenario suitable for application at abandoned sites or away from CO_2 generating sources. Scenario B aims to increase the concentration Mg^{2+} in the presence of a concentrated CO_2 stream, cation availability limits carbonation (Harrison et al., 2013; Power et al., 2014). Scenario B

can also increase dissolution of minerals and increase the availability of cations for carbonation (Daval et al., 2013; Power et al., 2014).

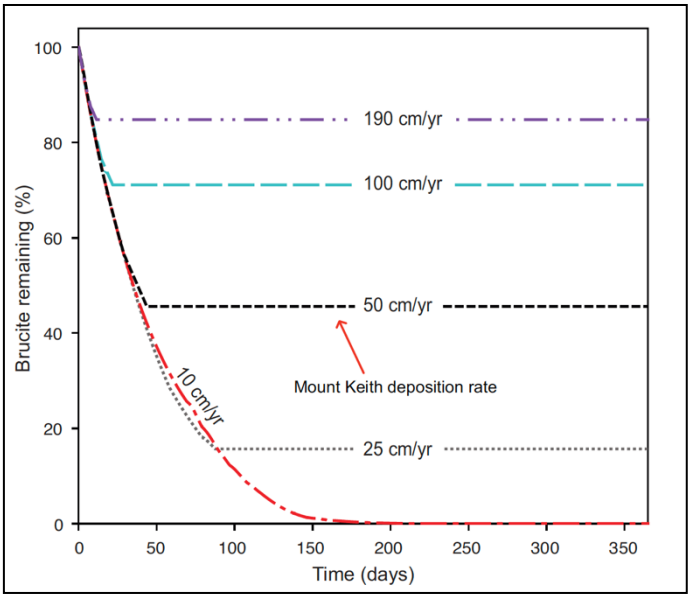

Fig. 5. MIN3P reactive transport modeling of Mount Keith tailings carbonation demonstrating the effect of tailings deposition rate on brucite carbonation. Reprinted from (Wilson et al., 2014). Copyright (2014) with permission from Elsevier.

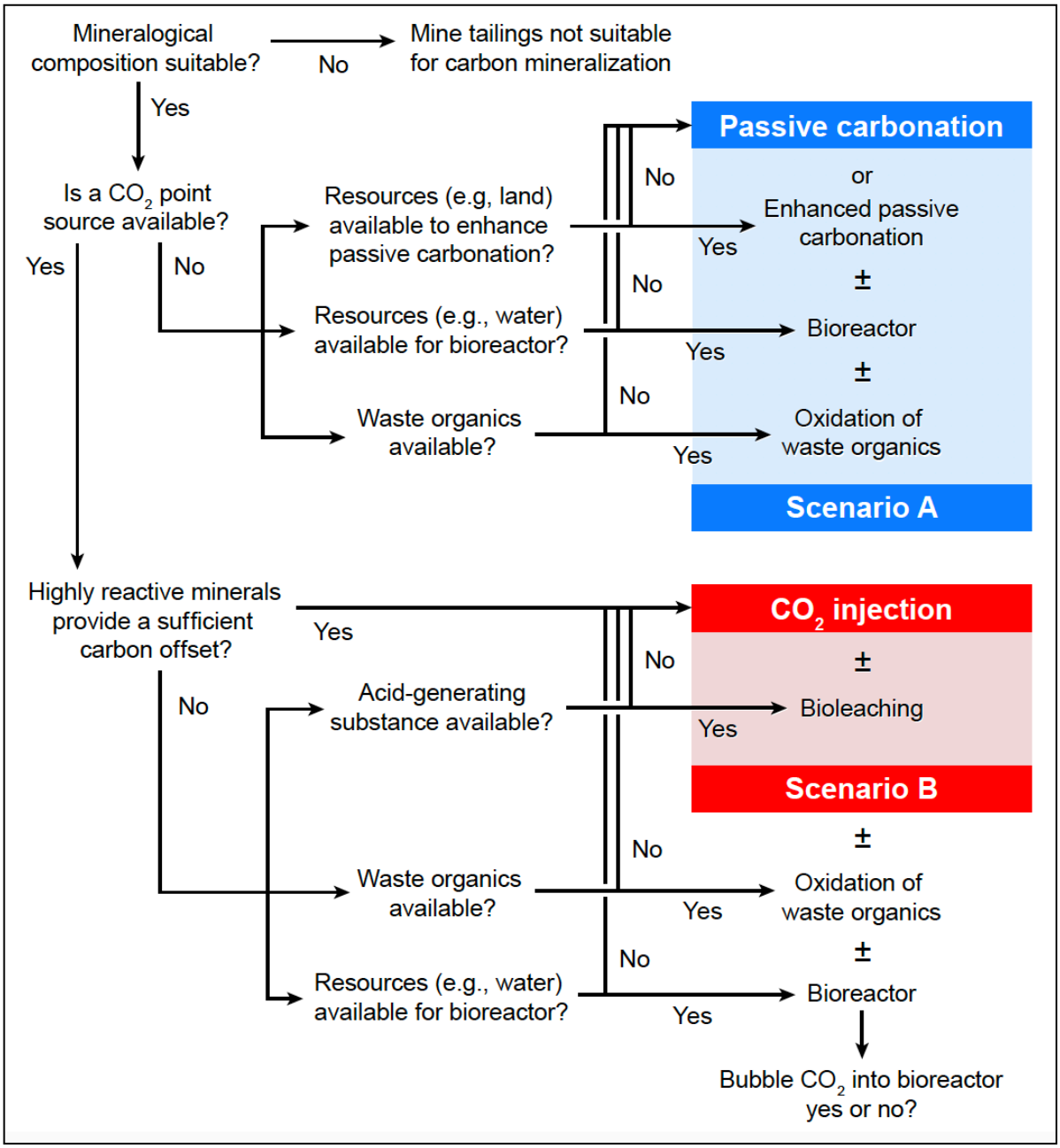

661 Fig. 6. Decision Tree for selecting mineral carbonation method. In Scenario A, CO_2 is captured from a
662 low-concentration stream such as the atmosphere, while in scenario B CO_2 is captured from a high-
663 concentration stream such as flue gas (Power et al., 2014). Reproduced from MDPI.

664 Finally, bacteria can be utilized to increase the CO_2 production within tailings.
665 McCutcheon et al. (2017) studied this increase by observing hydromagnesite
666 precipitation rates in two 0.5 m^3 passive carbonation cells, one of which was inoculated
667 with cyanobacteria. Over a period of 11 weeks, the weight fraction of hydromagnesite
668 reached 1.9% for the inoculated sample compared to 1.1% for the bacteria free
669 sample, in the top 2-4 cm of the tailings. For inoculated cells the CO_2 uptake reaches

137 g cm^{-2}, a rate that is much faster when compared to the control experiment in which CO_2 uptake was estimated to be 27 g cm^{-2} (McCutcheon et al., 2016).

5. Proposed large-scale passive CCS methods

As shown previously, alkaline wastes can be used as a carbon sink thereby providing a negative emissions solution. This section summarizes published work in which methods that can utilize passive carbonation on large scales were proposed, and it shows some results from their applications.

5.1 Direct air capture within designated cells

Abanades et al. (2020) proposed a system, composed of portlandite, that can capture CO_2 passively over a 6-month time scale, based on equations 8 (Renforth, 2019):

$$Ca(OH)_2 + CO_2 \rightarrow CaCO_3 \text{ , } \Delta G = -82.8 \text{ kJ/mol} \quad (8)$$

The proposed design can sequester 1 x 10^9 kg CO_2 per year by reacting it with 1.68 x 10^9 kg $Ca(OH)_2$. It is composed of multiple stacks of 2 x 2 x 0.03 m^3 plates composed of $Ca(OH)_2$ having a porosity of 0.5. Based on the reactions kinetics and air flow considerations, the proposed CCS system occupies a total volume of ~4.6 x 10^7 m^3, having a total area of ~4.6 x 10^6 m^2 and a height of ~10 m (Abanades et al., 2020).

The proposed design requires a volume that is one to two orders of magnitude larger than competitive, large-scale direct air capture systems. However, Abanades et al. (2020) argued that based on cost estimation proposed elsewhere (Guandalini et al., 2019), their proposed system is feasible. Their cost estimation considers different factors including the capital cost required for purchasing the oxy-combustion unit required for CaO production through calcination of $CaCO_3$, including fixed, variable

and fuel costs. Handling and transportation of structural elements, transporting the CO_2 produced during calcination to permanent storage as well as land cost were also incorporated in the cost estimation. They calculated that the cost of capturing 1000 kg of CO_2 through the proposed design ranges from US$ 138 - 341, a value that is significantly lower than the cost of US$ 600 / 1000 kg CO_2 reported by Climworks (Tollefson, 2018). At least 67% of this cost is allocated to the capture and storage of CO_2 produced through oxy-combustion of $CaCO_3$ which the authors considered to be the most appropriate source of $Ca(OH)_2$ that is used in the stacks.

McQueen et al. (2020) suggested an alternative process for direct air capture in which MgO is spread on land to capture CO_2 and form $MgCO_3$ spontaneously (ΔG = -75.9 kJ/mol (Renforth, 2019)). MgO is spread over a large area, and it reacts with CO_2 to produce $MgCO_3$. This process can remove between 6.0×10^{10} and 1.8×10^{11} $kgCO_2\ y^{-1}$, requiring an area of 4×10^8 - $1.1 \times 10^9\ m^2$, and it was estimated to cost 48-159 $ / 1000 $kgCO_2$. The provided cost includes the capital expenditure and operating expenditure, and the ranges reflect the uncertainties that are associated with the estimations of different variables, including calcination time and temperature, kiln efficiency, CO_2 uptake kinetics and capacity, energy prices and other economic factors. It should be noted that in the methods suggested by Abanades et al. (2020) and McQueen et al. (2020), CaO and MgO are assumed to be produced through calcination that produces a CO_2 stream, which is assumed to be stored elsewhere or sold. Clearly, the efficiency of these methods depends on the availability of points at which the produced CO_2 is either permanently stored or utilized in different applications.

5.2 Hot-stage carbonation

Another study proposed carbonation of slag, with flue gas, at an early stage immediately after the production and disposal of steel slag, in a process referred to as hot-stage carbonation (Santos et al., 2012). This process is based on enhancing the carbonation reaction by utilizing the hot temperature of slag to increase the reaction rate. To test this idea, BOF slag was subjected to calcination in order to remove any $CaCO_3$ that might have already formed, and then, using thermogravimetric analysis, the slag was cooled from 900 °C to 200 °C under CO_2 flowing at 100 ml/min in two different experiments: in the first one, the gas composition was 20% vol CO_2 as such a stream resembles a typical flue gas from iron and steel industry (Gielen, 2003). In the second experiment, the gas composition was set to 100% CO_2. Pressurization did not enhance CO_2 uptake significantly, and Santos et al. (2012) suggested it is more feasible to use CO_2 from flue gas for slag carbonation. Slag carbonation seemed to be diffusion-controlled as the CO_2 must diffuse through the inert constituent of the slag to the reactive site from the beginning of the carbonation process (Santos et al., 2012).

5.3 Reactivity enhancement by aqueous treatment

Alkaline pretreatment has been proposed to enhance leaching behavior and carbonation capacity of slag (Chen et al., 2019). The proposed carbonation enhancement method involves pretreating slag with alkaline solution since, as shown in a previous study (You et al., 2011) and illustrated in Fig. 7, when slag comes into contact with water, a dense layer of aluminosilicates may form and inhibit the carbonation reaction. This layer can be broken down upon the addition of alkaline sources and then converted to hydrated calcium phases, thereby producing more phases that can be carbonated to $CaCO_3$ (Chen et al., 2019; Matsushita et al., 2000).

To confirm this hypothesis, TGA analysis was carried out to determine the extent of carbonation for raw slag, and of the one that was pretreated with 1 M NaOH at a liquid/solid ratio of 10 mL/g prior to a long term (4-weeks) humidification. By measuring the weight loss between 600 and 800 ºC, the amount of $CaCO_3$ can be calculated. It was demonstrated that the amount of CO_2 captured within the pretreated slag was higher, as demonstrated in the calcite formation which was 17.05 and 50.68 mg $CaCO_3$ g^{-1} slag, for the raw slag and pretreated slag, respectively.

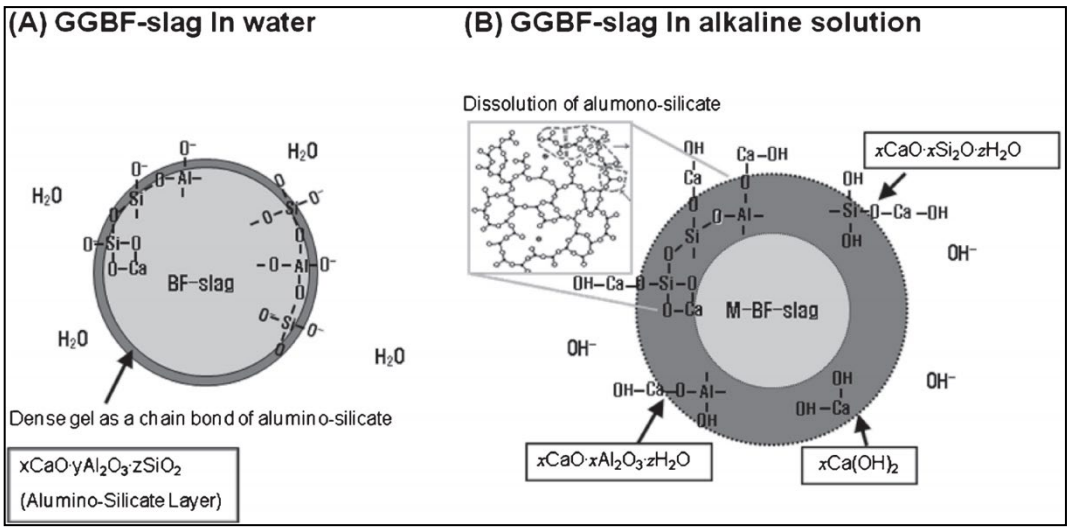

Fig. 7. Demonstration of alumino-silcate dissolution upon introducing NaOH to ground granulated blast furnace (GGBF) slag. Reprinted from You et al. (2011), Copyright (2011) with permission from The Japan Institute of Metals and Materials

Additionally, a waste management practice was proposed to enhance the carbonation, reduce leachate pH and allow for reactivity enhancement of the slag (Chen et al., 2019). Portrayed in Fig. 8, the method suggests placing the slag under a roof to limit the uncontrolled introduction of water. A geomembrane is also introduced to prevent leachate from reaching the surface beneath the slag. Finally, NaOH solution can be sprayed over the slag to enhance the carbonation reaction. This method, however, depends on the availability and cost of NaOH. Additionally, the emissions associated with NaOH manufacturing should also be considered to estimate the net CO_2 uptake through this process.

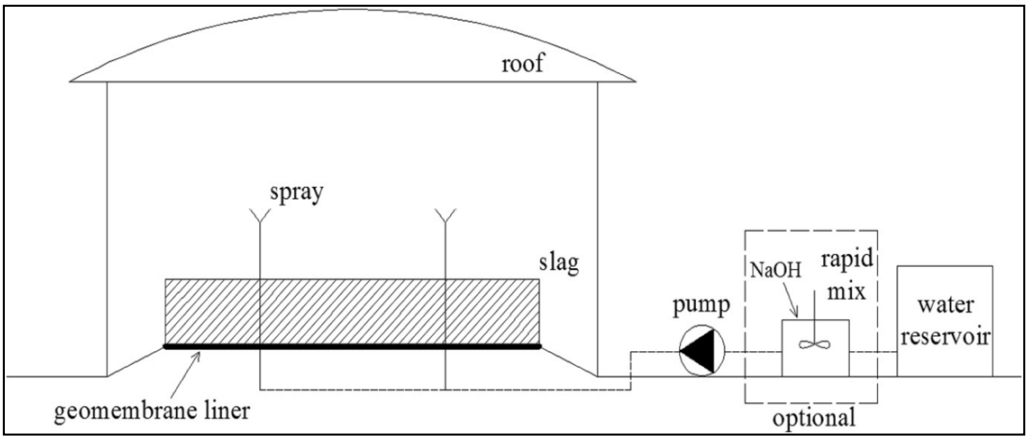

762 Fig. 8. Proposed slag carbonation method. Reprinted from (Chen et al., 2019). Copyright (2019) with
763 permission from Elsevier.

764 6. Points for future research

765 6.1 Economic valuation of passive carbonation

766 Understanding the economics of CCS projects provides incentives for
767 enterprises to develop CCS technologies and allow decision-makers to formulate
768 policies that promote development for CCS technologies (J. Li et al., 2019). As
769 explained earlier, there are several methods that can enhance mineral carbonation,
770 and implementing them is associated with the cost related to area requirement, size
771 reduction and establishing and maintaining piping systems for CO_2 delivery (Song et
772 al., 2021; Wilson et al., 2014). There is a lack in understanding the economics of
773 passive mineral carbonation. Valuation of carbon capture projects has been carried
774 using different methodologies, including optimization models, process simulation and
775 real options valuation (J. Li et al., 2019). One interesting method is the real options
776 (RO) valuation (Dixit and Pindyck, 2012), which is considered as a continuation of
777 financial options theory in that “firms with discretionary investment opportunities have
778 the right—but are under no obligation—to acquire expected cash flows by making an
779 investment on or before the date that the (investment) opportunity ceases to exist
780 (Glantz and Mun, 2011).” RO valuation has been used to study CCS projects,

considering several sources of uncertainties, such as policy, carbon prices, government incentive, and technological changes, as summarized by (H. Li et al., 2019) and the references therein. Additionally, it has been applied to CCS projects that involve CO_2 storage in geological formations or through using amine solution to absorb CO_2 (Ding et al., 2020; J. Li et al., 2019).

To our knowledge, only a single study (Power et al., 2014) explained about using RO to evaluate passive CO_2 mineralization projects. Investment in CCS technologies should be evaluated through the RO valuation since by doing so, a company can develop such technologies even when the CO_2 price is low, and it will have the right, but not the obligation, to apply such technologies when the CO_2 price becomes more accurate, and CCS becomes economically beneficial (Power et al., 2014). Passive carbonation is simple compared to other carbon capture technologies, and as such can have relatively low operation and transportation costs. Research on techno-economical evaluation can give confidence for mining companies to invest and apply passive carbonation techniques, and it provides an area of fundamental research.

6.2 Mobility of transition elements

There have been several studies showing that mining wastes can be a vital source of different transition metals (Gomes et al., 2016). Nevertheless, it has been argued that carbonation of alkaline wastes may reduce their environmental burdens (Bobicki et al., 2012; Mayes et al., 2008b; Renforth, 2019). For example, Hamilton et al. (2018) analyzed the mobility of transition elements during passive weathering and CO_2 sequestration within the chrysotile deposits at Woodsreef. Upon weathering, dissolution of serpentine and brucite released these elements, however they were captured upon precipitation of carbonates, either by substituting the Mg and Fe atoms

of the hydromagnesite and pyroaurite, or by being physically trapped within carbonate cement (Hamilton et al., 2018). As there were no detectable concentrations of transition metals within the mine pit water, Hamilton et al. (2018) concluded that mineral carbonation did not release toxic metals. While Hamilton et al. (2018) demonstrated that carbonates formed during CO_2 mineralization can also sequester transition metals, they also mentioned other issues that should be highlighted in future research. For example, hydrated carbonate such as nesquehonite transform to hydromagnesite and then to magnesite. It is not clear how this transformation affects the sequestered metals. Additionally, Mayes et al. (2008b) recommended examining the long-term stability of these metals in different precipitates under different conditions. Carbonation of other alkaline wastes may have different consequences on metals leaching. For example, the carbonation of slag was found to have a mixed effect on metals leaching – it decreased the leaching of barium, nickel and cobalt though it increased the leaching of chromium and vanadium (Santos et al., 2012). The carbonation of different alkaline wastes leads to the precipitation of different carbonates such as calcite, which may interact differently with ecotoxic metals, presenting an avenue for future research.

6.3 Life cycle assessment (LCA) consideration

LCA is a scientific method that evaluates the environmental impact of a process, quantitatively and qualitatively, throughout its life span (Li et al., 2022). LCA analysis measures different environmental impacts, such as air pollution, global warming, ecological toxicity, waste generation and resources depletion associated with a particular process, to ensure that it can actually solve an environmental problem rather than shifting it to another problem (Kikuchi, 2016). For example, Butera et al. (2015) highlighted that when demolition wastes are used in an unbound form, metals may

leach out and pollute the environment. Butera et al. (2015) highlighted that when LCA studies are performed, leaching is not always considered, or the used data may not reflect actual leaching behavior. Nevertheless, as carbonation of construction and demolition wastes may lower the leaching of metals, Butera et al. (2015) suggested that further research should be directed toward this issue to provide better understanding of environmental impacts associated with the carbonation of demolition wastes.

The physical properties of alkaline wastes may dictate having auxiliary operations such as crushing and transportation (Collins, 2010). Such steps may cause mineral carbonation to be less effective compared to geological sequestration and to cause other environmental problems (Giannoulakis et al., 2014). To our knowledge, however, there are limited LCA studies that evaluate the environmental impact of waste management practices that can enhance passive carbonation. For example, using flue gas to carbonate slag requires less transportation since both materials are produced in close locations, but may result in other emissions that are associated with maintaining and operating a CO_2 piping system as well as slag pulverization. LCA can assist in understanding the overall CO_2 uptake through this carbonation route and comparing it to other methods. Unlike mine waste, slag is produced at a larger size, and it must be pulverized before carbonation can take place. This makes mining wastes “low hanging fruits” as described by Kelemen et al. (2020), since they are already produced with large surface area as a consequence of mineral processing.

Finally, it should be noted that current LCA models require the calculation of the amount of industrial wastes that must be treated to capture a given amount of CO_2. This information can be calculated from the reaction rate laws that are available in the literature (e.g., Chang et al. (2013); Thom et al. (2013)). However, some interactions

between the operating conditions can result in unexpected CO_2 uptake. For example, Polettini et al. (2016b) demonstrated that under 1 bar 50 ºC and 40% CO_2, steel slag can capture CO_2 at an amount of 30 g CO_2/100g slag compared to 33 g CO_2/100 g slag captured under more elevated conditions of 10 bar, 100% CO_2 and 100 ºC. This indicates that there is room for further kinetic analysis of carbonation since the reduction of operating conditions and CO_2 concentration reduces the environmental impact of the mineral carbonation process.

7. Concluding remarks

There is growing evidence indicating that passive carbonation of alkaline wastes occurs to an extent that can reduce or offset the amount of CO_2 emitted from energy-intensive industries, such as steelmaking and mining. Globally, alkaline wastes are produced at a rate of 7×10^{12} - 1.7×10^{13} kg y^{-1} and by 2100, they are estimated to have an annual CO_2 capture potential of 2.9×10^{12} to 8.5×10^{12} kg y^{-1} (Renforth, 2019). However, studies show that the CO_2 uptake potential of alkaline wastes is underutilized due to several factors such as slow dissolution kinetics of silicate minerals, low CO_2 ingress into alkaline wastes and due to the passivation of reactive surfaces as a result of silica gel polymerization and carbonates precipitation. These challenges can be overcome through the application of different waste management practices such as controlling waste deposition rate, controlling the water saturation and the watering frequency and enhancing the contact between these wastes and the atmosphere. While the reviewed literature demonstrates that these methods can result in larger CO_2 uptake, the proposed methods should be evaluated through lifecycle assessment, which in turn requires adequate knowledge of leaching mechanisms of different ecotoxic metals that reside in the alkaline wastes. Although the proposed waste management practices are simple, they are associated with different costs

related to the area footprint and maintenance of CO_2 piping systems. Consequently, they should be evaluated from a techno-economic perspective.

Acknowledgement

Faisal W. K. Khudhur acknowledges generous support from the University of Glasgow Lord Kelvin/Adam Smith Ph.D. scholarship. Three anonymous reviewers are acknowledged for their comments that significantly enhanced this manuscript.

8. References

Abanades, J.C., Criado, Y.A., Fernández, J.R., 2020. An air CO2 capture system based on the passive carbonation of large Ca(OH)2 structures. Sustain. Energy Fuels 4, 3409–3417. https://doi.org/10.1039/D0SE00094A

Alcoa, 2012. Long Term Residue Management Strategy Kwinana 2012 [WWW Document]. URL https://www.alcoa.com/australia/en/pdf/kwinana_refinery_ltrms_report_2012.pdf (accessed 12.25.21).

Amiotte Suchet, P., Probst, J.-L., Ludwig, W., 2003. Worldwide distribution of continental rock lithology: Implications for the atmospheric/soil CO 2 uptake by continental weathering and alkalinity river transport to the oceans. Global Biogeochem. Cycles 17. https://doi.org/10.1029/2002GB001891

Archer, D., 2007. Global Warming: Understanding the Forecast, 1st ed. Blackwell Publishing.

Assima, G.P., Larachi, F., Beaudoin, G., Molson, J., 2013. Dynamics of carbon dioxide uptake in chrysotile mining residues – Effect of mineralogy and liquid saturation. Int. J. Greenh. Gas Control 12, 124–135. https://doi.org/10.1016/J.IJGGC.2012.10.001

Assima, G.P., Larachi, F., Beaudoin, G., Molson, J., 2012. CO2 Sequestration in Chrysotile Mining Residues—Implication of Watering and Passivation under Environmental Conditions. Ind. Eng. Chem. Res. 51, 8726–8734. https://doi.org/10.1021/IE202693Q

Assima, G.P., Larachi, F., Molson, J., Beaudoin, G., 2014a. Impact of temperature and oxygen availability on the dynamics of ambient CO2 mineral sequestration by nickel mining residues. Chem. Eng. J. 240, 394–403. https://doi.org/10.1016/J.CEJ.2013.12.010

Assima, G.P., Larachi, F., Molson, J., Beaudoin, G., 2014b. New tools for stimulating dissolution and carbonation of ultramafic mining residues. Can. J. Chem. Eng. 92, 2029–2038. https://doi.org/10.1002/CJCE.22066

Azdarpour, A., Asadullah, M., Mohammadian, E., Hamidi, H., Junin, R., Karaei, M.A., 2015. A review on carbon dioxide mineral carbonation through pH-swing process. Chem. Eng. J. 279, 615–630. https://doi.org/10.1016/J.CEJ.2015.05.064

Baker, D.R., Mancini, L., Polacci, M., Higgins, M.D., Gualda, G.A.R., Hill, R.J., Rivers, M.L., 2012. An introduction to the application of X-ray microtomography to the three-dimensional study of igneous rocks. Lithos 148, 262–276. https://doi.org/10.1016/j.lithos.2012.06.008

Bea, S.A., Wilson, S.A., Mayer, K.U., Dipple, G.M., Power, I.M., Gamazo, P., 2012. Reactive

921 Transport Modeling of Natural Carbon Sequestration in Ultramafic Mine Tailings.
922 Vadose Zo. J. 11, vzj2011.0053. https://doi.org/10.2136/vzj2011.0053
923 Beinlich, A., Austrheim, H., 2012. In situ sequestration of atmospheric CO 2 at low
924 temperature and surface cracking of serpentinized peridotite in mine shafts. Chem.
925 Geol. 332–333, 32–44. https://doi.org/10.1016/j.chemgeo.2012.09.015
926 Bobicki, E.R., Liu, Q., Xu, Z., Zeng, H., 2012. Carbon capture and storage using alkaline
927 industrial wastes. Prog. Energy Combust. Sci. 38, 302–320.
928 https://doi.org/10.1016/j.pecs.2011.11.002
929 Bodor, M., Santos, R.M., Kriskova, L., Elsen, J., Vlad, M., Van Gerven, T., 2013. Susceptibility
930 of mineral phases of steel slags towards carbonation: mineralogical, morphological and
931 chemical assessment. Eur. J. Mineral. 533–549. https://doi.org/10.1127/0935-
932 1221/2013/0025-2300
933 Boone, M.A., Nielsen, P., De Kock, T., Boone, M.N., Quaghebeur, M., Cnudde, V., 2014.
934 Monitoring of Stainless-Steel Slag Carbonation Using X-ray Computed
935 Microtomography. Environ. Sci. Technol. 48, 674–680.
936 https://doi.org/10.1021/es402767q
937 Brown, R., Brownlow, J., Krynen, J., 1992. Manilla - Narrabri 1:250000 Metallogenic Map,
938 SH/56-9, SH/55-12: Metallogenic Study and Mineral Deposit Data Sheets. NSW Geol.
939 Surv., Metallogenic Map. Ser.
940 Brown, T.J., Idoine, N.E., Wrighton, E.R., Raycraft, E.R., Hobbs, S.F., Shaw, R.A., Everett, P.,
941 Kresse, C., Deady, E.A., Bide, T., 2020. World Mineral Production 2014-2018 [WWW
942 Document]. Br. Geol. Surv. URL
943 https://www2.bgs.ac.uk/mineralsUK/statistics/worldStatistics.html
944 Buis, A., 2019. The Atmosphere: Getting a Handle on Carbon Dioxide – Climate Change: Vital
945 Signs of the Planet [WWW Document]. URL https://climate.nasa.gov/news/2915/the-
946 atmosphere-getting-a-handle-on-carbon-dioxide/ (accessed 1.18.22).
947 Bullock, L.A., Yang, A., Darton, R.C., 2022. Kinetics-informed global assessment of mine
948 tailings for CO2 removal. Sci. Total Environ. 808, 152111.
949 https://doi.org/10.1016/J.SCITOTENV.2021.152111
950 Butera, S., Christensen, T.H., Astrup, T.F., 2015. Life cycle assessment of construction and
951 demolition waste management. Waste Manag. 44, 196–205.
952 https://doi.org/10.1016/J.WASMAN.2015.07.011
953 Chang, E.E., Chiu, A.C., Pan, S.Y., Chen, Y.H., Tan, C.S., Chiang, P.C., 2013. Carbonation of
954 basic oxygen furnace slag with metalworking wastewater in a slurry reactor. Int. J.
955 Greenh. Gas Control 12, 382–389. https://doi.org/10.1016/j.ijggc.2012.11.026
956 Chang, E.E., Pan, S.Y., Chen, Y.H., Tan, C.S., Chiang, P.C., 2012. Accelerated carbonation of
957 steelmaking slags in a high-gravity rotating packed bed. J. Hazard. Mater. 227–228, 97–
958 106. https://doi.org/10.1016/j.jhazmat.2012.05.021
959 Chen, B., Yoon, S., Zhang, Y., Han, L., Choi, Y., 2019. Reduction of steel slag leachate pH via
960 humidification using water and aqueous reagents. Sci. Total Environ. 671, 598–607.
961 https://doi.org/10.1016/j.scitotenv.2019.03.362
962 Chiang, P.C., Pan, S.Y., 2017. Carbon dioxide mineralization and utilization, Carbon Dioxide
963 Mineralization and Utilization. https://doi.org/10.1007/978-981-10-3268-4
964 Chukwuma, J.S., Pullin, H., Renforth, P., 2021. Assessing the carbon capture capacity of
965 South Wales' legacy iron and steel slag. Miner. Eng. 173, 107232.
966 https://doi.org/10.1016/J.MINENG.2021.107232
967 Collins, F., 2010. Inclusion of carbonation during the life cycle of built and recycled concrete:

968 Influence on their carbon footprint. Int. J. Life Cycle Assess. 15, 549–556.
969 https://doi.org/10.1007/S11367-010-0191-4/TABLES/5
970 Daval, D., 2018. Carbon dioxide sequestration through silicate degradation and carbon
971 mineralisation: promises and uncertainties. npj Mater. Degrad. 2, 1–4.
972 https://doi.org/10.1038/s41529-018-0035-4
973 Daval, D., Hellmann, R., Martinez, I., Gangloff, S., Guyot, F., 2013. Lizardite serpentine
974 dissolution kinetics as a function of pH and temperature, including effects of elevated
975 pCO2. Chem. Geol. 351, 245–256. https://doi.org/10.1016/j.chemgeo.2013.05.020
976 Daval, D., Martinez, I., Corvisier, J., Findling, N., Goffé, B., Guyot, F., 2009. Carbonation of
977 Ca-bearing silicates, the case of wollastonite: Experimental investigations and kinetic
978 modeling. Chem. Geol. 265, 63–78. https://doi.org/10.1016/J.CHEMGEO.2009.01.022
979 Dembicki, Jr., H., 2017. Source Rock Evaluation, in: Practical Petroleum Geochemistry for
980 Exploration and Production. Elsevier, pp. 61–133. https://doi.org/10.1016/B978-0-12-
981 803350-0.00003-9
982 Ding, H., Zheng, H., Liang, X., Ren, L., 2020. Getting ready for carbon capture and storage in
983 the iron and steel sector in China: Assessing the value of capture readiness. J. Clean.
984 Prod. 244, 118953. https://doi.org/10.1016/j.jclepro.2019.118953
985 Dixit, A.K., Pindyck, R.S., 2012. Investment Under Uncertainty. Princeton University Press.
986 Dlugogorski, B.Z., Balucan, R.D., 2014. Dehydroxylation of serpentine minerals: Implications
987 for mineral carbonation. Renew. Sustain. Energy Rev. 31, 353–367.
988 https://doi.org/10.1016/J.RSER.2013.11.002
989 Edwards, K.J., Goebel, B.M., 1999. Geomicrobiology of Pyrite (FeS2) Dissolution: Case Study
990 at Iron Mountain, California. Geomicrobiol. J. 16, 155–179.
991 https://doi.org/10.1080/014904599270668
992 Engström, F., Adolfsson, D., Samuelsson, C., Sandström, Å., Björkman, B., 2013. A study of
993 the solubility of pure slag minerals. Miner. Eng. 41, 46–52.
994 https://doi.org/10.1016/J.MINENG.2012.10.004
995 Gaillardet, J., Dupré, B., Louvat, P., Allègre, C.J., 1999. Global silicate weathering and CO2
996 consumption rates deduced from the chemistry of large rivers. Chem. Geol. 159, 3–30.
997 https://doi.org/10.1016/S0009-2541(99)00031-5
998 Gao, X., Jiang, L., Mao, Y., Yao, B., Jiang, P., 2021. Progress, Challenges, and Perspectives of
999 Bioleaching for Recovering Heavy Metals from Mine Tailings. Adsorpt. Sci. Technol.
1000 2021. https://doi.org/10.1155/2021/9941979
1001 Gencel, O., Karadag, O., Oren, O.H., Bilir, T., 2021. Steel slag and its applications in cement
1002 and concrete technology: A review. Constr. Build. Mater. 283, 122783.
1003 https://doi.org/10.1016/j.conbuildmat.2021.122783
1004 Geoscience Australia, 2018. Aluminium [WWW Document]. URL
1005 https://www.ga.gov.au/education/classroom-resources/minerals-energy/australian-
1006 mineral-facts/aluminium (accessed 10.11.20).
1007 Giannoulakis, S., Volkart, K., Bauer, C., 2014. Life cycle and cost assessment of mineral
1008 carbonation for carbon capture and storage in European power generation. Int. J.
1009 Greenh. Gas Control 21, 140–157. https://doi.org/10.1016/j.ijggc.2013.12.002
1010 Gielen, D., 2003. CO2 removal in the iron and steel industry. Energy Convers. Manag. 44,
1011 1027–1037. https://doi.org/10.1016/S0196-8904(02)00111-5
1012 Glantz, M., Mun, J., 2011. Introduction, in: Credit Engineering for Bankers. Elsevier, pp. xvii–
1013 xxi. https://doi.org/10.1016/B978-0-12-378585-5.10027-2
1014 Goetz, E.R., Riefler, R.G., 2015. Geochemistry of CO2 in Steel Slag Leach Beds. Mine Water

Environ. 34, 42–49. https://doi.org/10.1007/s10230-014-0290-8
Gomes, H.I., Mayes, W.M., Rogerson, M., Stewart, D.I., Burked, I.T., 2016. Alkaline residues and the environment: A review of impacts, management practices and opportunities. J. Clean. Prod. https://doi.org/10.1016/j.jclepro.2015.09.111
Gore, M., 2015. Geotechnical Characterization of Bauxite Residue. The University of Texas at Austin.
Gras, A., Beaudoin, G., Molson, J., Plante, B., 2020. Atmospheric carbon sequestration in ultramafic mining residues and impacts on leachate water chemistry at the Dumont Nickel Project, Quebec, Canada. Chem. Geol. 546, 119661. https://doi.org/10.1016/j.chemgeo.2020.119661
Gras, A., Beaudoin, G., Molson, J., Plante, B., Bussière, B., Lemieux, J.M., Dupont, P.P., 2017. Isotopic evidence of passive mineral carbonation in mine wastes from the Dumont Nickel Project (Abitibi, Quebec). Int. J. Greenh. Gas Control 60, 10–23. https://doi.org/10.1016/j.ijggc.2017.03.002
Gras, A., Beaudoin, G., Molson, J., Plante, B., Bussière, B., Lemieux, J.M., Kandji, B., 2015. Carbon isotope evidence for passive mineral carbonation of mine wastes from the Dumont Nickel Project (Abitibi, Quebec) - ACEME 2015, in: 5th International Conference on Accelerated Carbonation for Environmental and Material Engineering. New York, USA.
Grénman, H., Ramirez, F., Eränen, K., Wärnå, J., Salmi, T., Murzin, D.Y., 2008. Dissolution of Mineral Fiber in a Formic Acid Solution: Kinetics, Modeling, and Gelation of the Resulting Sol. Ind. Eng. Chem. Res. 47, 9834–9841. https://doi.org/10.1021/IE800267A
Guandalini, G., Romano, M.C., Ho, M., Wiley, D., Rubin, E.S., Abanades, J.C., 2019. A sequential approach for the economic evaluation of new CO2 capture technologies for power plants. Int. J. Greenh. Gas Control 84, 219–231. https://doi.org/10.1016/j.ijggc.2019.03.006
Gunning, P.J., Hills, C.D., Carey, P.J., 2010. Accelerated carbonation treatment of industrial wastes. Waste Manag. 30, 1081–1090. https://doi.org/10.1016/j.wasman.2010.01.005
Hamilton, J.L., Wilson, S.A., Morgan, B., Turvey, C.C., Paterson, D.J., Jowitt, S.M., McCutcheon, J., Southam, G., 2018. Fate of transition metals during passive carbonation of ultramafic mine tailings via air capture with potential for metal resource recovery. Int. J. Greenh. Gas Control 71, 155–167. https://doi.org/10.1016/j.ijggc.2018.02.008
Hamilton, J.L., Wilson, S.A., Turvey, C.C., Tait, A.W., McCutcheon, J., Fallon, S.J., Southam, G., (In prep). Field-based deployment of an automated geochemical treatment system for accelerating carbonation of ultramafic mine tailings: Lessons for pilot projects and carbon accounting in mined landscapes. In Preparation.
Han, Y.-S., Ji, S., Lee, P.-K., Oh, C., 2017. Bauxite residue neutralization with simultaneous mineral carbonation using atmospheric CO2. J. Hazard. Mater. 326, 87–93. https://doi.org/10.1016/j.jhazmat.2016.12.020
Harnisch, J., Wing, I.S., Jacoby, H.D., Prinn, R.G., 1998. Primary Aluminum Production: Climate Policy, Emissions and Costs. Joint Program Report Series 44.
Harrison, A.L., Power, I.M., Dipple, G.M., 2013. Strategies for enhancing carbon sequestration in Mg-rich mine tailings, in: Wolkersdorfer, Brown, Figueroa (Eds.), IMWA: Reliable Mine Water Technology. IMWA, Golden Coloradon, USA.
Harrison, A.L., Power, I.M., Dipple, G.M., 2012. Accelerated Carbonation of Brucite in Mine Tailings for Carbon Sequestration. Environ. Sci. Technol. 47, 126–134.

https://doi.org/10.1021/ES3012854
Hu, R., Xie, J., Wu, S., Yang, C., Yang, D., 2020. Study of toxicity assessment of heavy metals from steel slag and its asphalt mixture. Materials (Basel). 13, 2768. https://doi.org/10.3390/ma13122768
Huh, Y., 2003. Chemical weathering and climate — a global experiment: A review. Geosci. J. 7, 277–288. https://doi.org/10.1007/BF02910294
Huijgen, W.J.J., Comans, R.N.J., 2005. Carbon dioxide sequestration by mineral carbonation: Literature review update 2003-2004.
Huijgen, W.J.J., Witkamp, G.J., Comans, R.N.J., 2005. Mineral CO2 sequestration by steel slag carbonation. Environ. Sci. Technol. 39, 9676–9682. https://doi.org/10.1021/es050795f
Indian and Northern Affairs Canada, 2008. The Big Picture Yukon's Large Contaminated Sites [WWW Document]. URL https://www.aadnc-aandc.gc.ca/DAM/DAM-INTER-YT/STAGING/texte-text/pubs-tbp-pdf_1316463525304_eng.pdf (accessed 3.11.21).
IPCC, 2021. Summary for Policymakers. In: Climate Change 2021: The Physical Science Basis. Contribution of Working Group I to the Sixth Assessment Report of the Intergovernmental Panel on Climate Change.
Jorat, M.E., Goddard, M.A., Manning, P., Lau, H.K., Ngeow, S., Sohi, S.P., Manning, D.A.C., 2020. Passive CO2 removal in urban soils: Evidence from brownfield sites. Sci. Total Environ. 703, 135573. https://doi.org/10.1016/j.scitotenv.2019.135573
Kandji, E.H.B., Plante, B., Bussière, B., Beaudoin, G., Dupont, P.P., 2017. Kinetic testing to evaluate the mineral carbonation and metal leaching potential of ultramafic tailings: Case study of the Dumont Nickel Project, Amos, Québec. Appl. Geochemistry 84, 262–276. https://doi.org/10.1016/j.apgeochem.2017.07.005
Kelemen, P.B., Matter, J., Streit, E.E., Rudge, J.F., Curry, W.B., Blusztajn, J., 2011. Rates and mechanisms of mineral carbonation in peridotite: Natural processes and recipes for enhanced, in situ CO2 capture and storage. Annu. Rev. Earth Planet. Sci. 39, 545–576. https://doi.org/10.1146/annurev-earth-092010-152509
Kelemen, P.B., McQueen, N., Wilcox, J., Renforth, P., Dipple, G., Vankeuren, A.P., 2020. Engineered carbon mineralization in ultramafic rocks for CO2 removal from air: Review and new insights. Chem. Geol. 550, 119628. https://doi.org/10.1016/j.chemgeo.2020.119628
Khaitan, S., Dzombak, D.A., Swallow, P., Schmidt, K., Fu, J., Lowry, G. V, 2010. Field Evaluation of Bauxite Residue Neutralization by Carbon Dioxide, Vegetation, and Organic Amendments. J. Environ. Eng. 136, 1045–1053. https://doi.org/10.1061/(ASCE)EE.1943-7870.0000230
Kikuchi, Y., 2016. Life Cycle Assessment, in: Plant Factory: An Indoor Vertical Farming System for Efficient Quality Food Production. Academic Press, pp. 321–329. https://doi.org/10.1016/B978-0-12-801775-3.00024-X
Kriskova, L., Pontikes, Y., Pandelaers, L., Cizer, Ö., Jones, P.T., Van Balen, K., Blanpain, B., 2013. Effect of High Cooling Rates on the Mineralogy and Hydraulic Properties of Stainless Steel Slags. Metall. Mater. Trans. B 2013 445 44, 1173–1184. https://doi.org/10.1007/S11663-013-9894-9
Lai, J.L., Shek, C.H., Ho Lo, K., 2012. Stainless Steel An Introduction and Their Recent Developments : An Introduction and Their Recent Developments. Bentham Science Publishers, ProQuest Ebook Central, https://ebookcentral.proquest.com/lib/gla/detail.action?docID=877022.
Lechat, K., Lemieux, J.M., Molson, J., Beaudoin, G., Hébert, R., 2016. Field evidence of CO2

sequestration by mineral carbonation in ultramafic milling wastes, Thetford Mines, Canada. Int. J. Greenh. Gas Control 47, 110–121. https://doi.org/10.1016/j.ijggc.2016.01.036

LECO Corporation, 2008. SC-144DR Sulfur/Carbon Determinator Specification Sheet.

Li, H., Jiang, H.D., Yang, B., Liao, H., 2019. An analysis of research hotspots and modeling techniques on carbon capture and storage. Sci. Total Environ. 687, 687–701. https://doi.org/10.1016/j.scitotenv.2019.06.013

Li, J., Hou, Y., Wang, P., Yang, B., 2019. A Review of carbon capture and storage project investment and operational decision-making based on bibliometrics. Energies 12. https://doi.org/10.3390/en12010023

Li, L., Ling, T.-C., Pan, S.-Y., 2022. Environmental benefit assessment of steel slag utilization and carbonation: A systematic review. Sci. Total Environ. 806, 150280. https://doi.org/10.1016/j.scitotenv.2021.150280

Liu, W., Teng, L., Rohani, S., Qin, Z., Zhao, B., Xu, C.C., Ren, S., Liu, Q., Liang, B., 2021. CO2 mineral carbonation using industrial solid wastes: A review of recent developments. Chem. Eng. J. 416, 129093. https://doi.org/10.1016/J.CEJ.2021.129093

Marinković, S.B., Malešev, M., Ignjatović, I., 2014. Life cycle assessment (LCA) of concrete made using recycled concrete or natural aggregates. Eco-Efficient Constr. Build. Mater. Life Cycle Assess. (LCA), Eco-Labelling Case Stud. 239–266. https://doi.org/10.1533/9780857097729.2.239

Matsushita, F., Aono, Y., Shibata, S., 2000. Carbonation degree of autoclaved aerated concrete. Cem. Concr. Res. 30, 1741–1745. https://doi.org/10.1016/S0008-8846(00)00424-5

Mayes, W.M., Gozzard, E., Potter, H.A.B., Jarvis, A.P., 2008a. Quantifying the importance of diffuse minewater pollution in a historically heavily coal mined catchment. Environ. Pollut. 151, 165–175. https://doi.org/10.1016/j.envpol.2007.02.008

Mayes, W.M., Jarvis, A.P., Burke, I.T., Walton, M., Feigl, V., Klebercz, O., Gruiz, K., 2011. Dispersal and Attenuation of Trace Contaminants Downstream of the Ajka Bauxite Residue (Red Mud) Depository Failure, Hungary. Environ. Sci. Technol. 45, 5147–5155. https://doi.org/10.1021/es200850y

Mayes, W.M., Riley, A.L., Gomes, H.I., Brabham, P., Hamlyn, J., Pullin, H., Renforth, P., 2018. Atmospheric CO 2 Sequestration in Iron and Steel Slag: Consett, County Durham, United Kingdom. Environ. Sci. Technol. 52, 7892–7900. https://doi.org/10.1021/acs.est.8b01883

Mayes, W.M., Younger, P, L., Aumônier, J., 2006. Buffering of Alkaline Steel Slag Leachate across a Natural Wetland. Environ. Sci. Technol. 40, 1237–1243. https://doi.org/10.1021/ES051304U

Mayes, W.M., Younger, P.L., Aumônier, J., 2008b. Hydrogeochemistry of alkaline steel slag leachates in the UK. Water. Air. Soil Pollut. 195, 35–50. https://doi.org/10.1007/S11270-008-9725-9/TABLES/4

McCutcheon, J., Turvey, C.C., Wilson, S.A., Hamilton, J.L., Southam, G., 2017. Experimental deployment of microbial mineral carbonation at an asbestos mine: Potential applications to carbon storage and tailings stabilization. Minerals 7, 15–18. https://doi.org/10.3390/min7100191

McCutcheon, J., Wilson, S.A., Southam, G., 2016. Microbially Accelerated Carbonate Mineral Precipitation as a Strategy for in Situ Carbon Sequestration and Rehabilitation of Asbestos Mine Sites. Environ. Sci. Technol. 50, 1419–1427.

https://doi.org/10.1021/ACS.EST.5B04293
McQueen, N., Kelemen, P., Dipple, G., Renforth, P., Wilcox, J., 2020. Ambient weathering of magnesium oxide for CO2 removal from air. Nat. Commun. 2020 111 11, 1–10. https://doi.org/10.1038/s41467-020-16510-3
Mervine, E.M., Wilson, S.A., Power, I.M., Dipple, G.M., Turvey, C.C., Hamilton, J.L., Vanderzee, S., Raudsepp, M., Southam, C., Matter, J.M., Kelemen, P.B., Stiefenhofer, J., Miya, Z., Southam, G., 2018. Potential for offsetting diamond mine carbon emissions through mineral carbonation of processed kimberlite: an assessment of De Beers mine sites in South Africa and Canada. Mineral. Petrol. 112, 755–765. https://doi.org/10.1007/s00710-018-0589-4
Meyer, D.R., 1980. Nutritional problems associated with the establishment of vegetation on tailings from an asbestos mine. Environ. Pollut. Ser. A, Ecol. Biol. 23, 287–298. https://doi.org/10.1016/0143-1471(80)90071-9
Mitchel, R.H., 1986. Kimberlite and Related Rocks, in: Kimberlites Mineralogy, Geochemistry, and Petrology. Plenum Press, New York, USA, pp. 9–28.
Mukiza, E., Zhang, L.L., Liu, X., Zhang, N., 2019. Utilization of red mud in road base and subgrade materials: A review. Resour. Conserv. Recycl. https://doi.org/10.1016/j.resconrec.2018.10.031
National Academies of Sciences Engineering and Medicine, 2019. Negative Emissions Technologies and Reliable Sequestration. Washington DC. https://doi.org/10.17226/25259
Nordstrom, D.K., Southam, G., 1997. Geomicrobiology of sulfide mineral oxidation. Rev. Mineral. 35, 381–390. https://doi.org/10.1515/9781501509247
Nowamooz, A., Dupuis, J.C., Beaudoin, G., Molson, J., Lemieux, J.-M., Horswill, M., Fortier, R., Larachi, F., Maldague, X., Constantin, M., Duchesne, J., Therrien, R., 2018. Atmospheric Carbon Mineralization in an Industrial-Scale Chrysotile Mining Waste Pile. Environ. Sci. Technol. 52, 8050–8057. https://doi.org/10.1021/ACS.EST.8B01128
Olabi, A.G., Obaideen, K., Elsaid, K., Wilberforce, T., Sayed, E.T., Maghrabie, H.M., Abdelkareem, M.A., 2022. Assessment of the pre-combustion carbon capture contribution into sustainable development goals SDGs using novel indicators. Renew. Sustain. Energy Rev. 153, 111710. https://doi.org/10.1016/J.RSER.2021.111710
Olszewska, J.P., Meharg, A.A., Heal, K. V, Carey, M., Gunn, I.D.M., Searle, K.R., Winfield, I.J., Spears, B.M., 2016. Assessing the Legacy of Red Mud Pollution in a Shallow Freshwater Lake: Arsenic Accumulation and Speciation in Macrophytes. https://doi.org/10.1021/acs.est.6b00942
Oskierski, H.C., Dlugogorski, B.Z., Jacobsen, G., 2013. Sequestration of atmospheric CO2 in chrysotile mine tailings of the Woodsreef Asbestos Mine, Australia: Quantitative mineralogy, isotopic fingerprinting and carbonation rates. Chem. Geol. 358, 156–169. https://doi.org/10.1016/j.chemgeo.2013.09.001
Oskierski, H.C., Dlugogorski, B.Z., Oliver, T.K., Jacobsen, G., 2016. Chemical and isotopic signatures of waters associated with the carbonation of ultramafic mine tailings, Woodsreef Asbestos Mine, Australia. Chem. Geol. 436, 11–23. https://doi.org/10.1016/j.chemgeo.2016.04.014
Oskierski, H.C., Turvey, C.C., Wilson, S.A., Dlugogorski, B.Z., Altarawneh, M., Mavromatis, V., 2021. Mineralisation of atmospheric CO2 in hydromagnesite in ultramafic mine tailings – Insights from Mg isotopes. Geochim. Cosmochim. Acta 309, 191–208. https://doi.org/10.1016/J.GCA.2021.06.020

Pade, C., Guimaraes, M., 2007. The CO2 uptake of concrete in a 100 year perspective. Cem. Concr. Res. 37, 1348–1356. https://doi.org/10.1016/J.CEMCONRES.2007.06.009

Pan, S.Y., Chang, E.E., Chiang, P.C., 2012. CO2 capture by accelerated carbonation of alkaline wastes: A review on its principles and applications. Aerosol Air Qual. Res. 12, 770–791. https://doi.org/10.4209/aaqr.2012.06.0149

Paulo, C., Power, I.M., Stubbs, A.R., Wang, B., Zeyen, N., Wilson, S.A., 2021. Evaluating feedstocks for carbon dioxide removal by enhanced rock weathering and CO2 mineralization. Appl. Geochemistry 129, 104955. https://doi.org/10.1016/J.APGEOCHEM.2021.104955

Pokrovsky, O.S., Schott, J., 2000. Kinetics and mechanism of forsterite dissolution at 25°C and pH from 1 to 12. Geochim. Cosmochim. Acta 64, 3313–3325. https://doi.org/10.1016/S0016-7037(00)00434-8

Polettini, A., Pomi, R., Stramazzo, A., 2016. CO2 sequestration through aqueous accelerated carbonation of BOF slag: A factorial study of parameters effects. J. Environ. Manage. 167, 185–195. https://doi.org/10.1016/j.jenvman.2015.11.042

Power, G., Gräfe, M., Klauber, C., 2011. Bauxite residue issues: I. Current management, disposal and storage practices. Hydrometallurgy 108, 33–45. https://doi.org/10.1016/J.HYDROMET.2011.02.006

Power, I., McCutcheon, J., Harrison, A., Wilson, S., Dipple, G., Kelly, S., Southam, C., Southam, G., 2014. Strategizing Carbon-Neutral Mines: A Case for Pilot Projects. Minerals 4, 399–436. https://doi.org/10.3390/min4020399

Power, I.M., Dipple, G.M., Southam, G., 2010. Bioleaching of ultramafic tailings by Acidithiobacillus spp. for CO 2 sequestration. Environ. Sci. Technol. 44, 456–462. https://doi.org/10.1021/ES900986N/SUPPL_FILE/ES900986N_SI_001.PDF

Power, I.M., Harrison, A.L., Dipple, G.M., Wilson, S.A., Kelemen, P.B., Hitch, M., Southam, G., 2013. Carbon Mineralization: From Natural Analogues to Engineered Systems. Rev. Mineral. Geochemistry 77, 305–360. https://doi.org/10.2138/rmg.2013.77.9

Proctor, D.M., Fehling, K.A., Shay, E.C., Wittenborn, J.L., Green, J.J., Avent, C., Bigham, R.D., Connolly, M., Lee, B., Shepker, T.O., Zak, M.A., 2000. Physical and chemical characteristics of blast furnace, basic oxygen furnace, and electric arc furnace steel industry slags. Environ. Sci. Technol. 34, 1576–1582. https://doi.org/10.1021/es9906002

Pronost, J., Beaudoin, G., Constantin, M., Duchesne, J., Hébert, R., 2010. Evaluation of the mineral carbonation potential of mining residues produced by Royal Nickel pilot plant, Amos.

Pronost, J., Beaudoin, G., Lemieux, J.M., Hébert, R., Constantin, M., Marcouiller, S., Klein, M., Duchesne, J., Molson, J.W., Larachi, F., Maldague, X., 2012. CO2-depleted warm air venting from chrysotile milling waste (Thetford Mines, Canada): Evidence for in-situ carbon capture from the atmosphere. Geology 40, 275–278. https://doi.org/10.1130/G32583.1

Pullin, H., Bray, A.W., Burke, I.T., Muir, D.D., Sapsford, D.J., Mayes, W.M., Renforth, P., 2019. Atmospheric Carbon Capture Performance of Legacy Iron and Steel Waste. Environ. Sci. Technol. 53, 9502–9511. https://doi.org/10.1021/acs.est.9b01265

Ragipani, R., Bhattacharya, S., Suresh, A.K., 2021. A review on steel slag valorisation: Via mineral carbonation. React. Chem. Eng. 6, 1152–1178. https://doi.org/10.1039/d1re00035g

Renforth, P., 2019. The negative emission potential of alkaline materials. Nat. Commun. 10,

1401. https://doi.org/10.1038/s41467-019-09475-5
Renforth, P., 2011. Mineral carbonation in soils : engineering the soil carbon sink. University of New Castle.
Renforth, P., Manning, D.A.C., Lopez-Capel, E., 2009. Carbonate precipitation in artificial soils as a sink for atmospheric carbon dioxide. Appl. Geochemistry 24, 1757–1764. https://doi.org/10.1016/j.apgeochem.2009.05.005
Renforth, P., Mayes, W.M., Jarvis, A.P., Burke, I.T., Manning, D.A.C., Gruiz, K., 2012. Contaminant mobility and carbon sequestration downstream of the Ajka (Hungary) red mud spill: The effects of gypsum dosing. Sci. Total Environ. 421–422, 253–259. https://doi.org/10.1016/j.scitotenv.2012.01.046
Renforth, P., Washbourne, C.-L., Taylder, J., Manning, D.A.C., 2011. Silicate Production and Availability for Mineral Carbonation. Environ. Sci. Technol. 45, 2035–2041. https://doi.org/10.1021/es103241w
Riahi, K., van Vuuren, D.P., Kriegler, E., Edmonds, J., O'Neill, B.C., Fujimori, S., Bauer, N., Calvin, K., Dellink, R., Fricko, O., Lutz, W., Popp, A., Cuaresma, J.C., KC, S., Leimbach, M., Jiang, L., Kram, T., Rao, S., Emmerling, J., Ebi, K., Hasegawa, T., Havlik, P., Humpenöder, F., Da Silva, L.A., Smith, S., Stehfest, E., Bosetti, V., Eom, J., Gernaat, D., Masui, T., Rogelj, J., Strefler, J., Drouet, L., Krey, V., Luderer, G., Harmsen, M., Takahashi, K., Baumstark, L., Doelman, J.C., Kainuma, M., Klimont, Z., Marangoni, G., Lotze-Campen, H., Obersteiner, M., Tabeau, A., Tavoni, M., 2017. The Shared Socioeconomic Pathways and their energy, land use, and greenhouse gas emissions implications: An overview. Glob. Environ. Chang. 42, 153–168. https://doi.org/10.1016/j.gloenvcha.2016.05.009
Riley, A.L., MacDonald, J.M., Burke, I.T., Renforth, P., Jarvis, A.P., Hudson-Edwards, K.A., McKie, J., Mayes, W.M., 2020. Legacy iron and steel wastes in the UK: Extent, resource potential, and management futures. J. Geochemical Explor. 219, 106630. https://doi.org/10.1016/j.gexplo.2020.106630
Riley, A.L., Mayes, W.M., 2015. Long-term evolution of highly alkaline steel slag drainage waters. Environ. Monit. Assess. 187, 463. https://doi.org/10.1007/s10661-015-4693-1
Roadcap, G.S., Kelly, W.R., Bethke, C.M., 2005. Geochemistry of Extremely Alkaline (pH > 12) Ground Water in Slag-Fill Aquifers. Ground Water 43, 806–816. https://doi.org/10.1111/j.1745-6584.2005.00060.x
Roadcap, G.S., Sanford, R.A., Jin, Q., Pardinas, J.R., Bethke, C.M., 2006. Extremely alkaline (pH > 12) ground water hosts diverse microbial community. Ground Water 44, 511–517. https://doi.org/10.1111/j.1745-6584.2006.00199.x
Santini, T.C., Banning, N.C., 2016. Alkaline tailings as novel soil forming substrates: Reframing perspectives on mining and refining wastes. Hydrometallurgy 164, 38–47. https://doi.org/10.1016/j.hydromet.2016.04.011
Santos, R.M., Ling, D., Sarvaramini, A., Guo, M., Elsen, J., Larachi, F., Beaudoin, G., Blanpain, B., Van Gerven, T., 2012. Stabilization of basic oxygen furnace slag by hot-stage carbonation treatment. Chem. Eng. J. 203, 239–250. https://doi.org/10.1016/j.cej.2012.06.155
Schott, J., Pokrovsky, O.S., Oelkers, E.H., 2009. The Link Between Mineral Dissolution/Precipitation Kinetics and Solution Chemistry. Rev. Mineral. Geochemistry 70, 207–258. https://doi.org/10.2138/RMG.2009.70.6
Schott, J., Pokrovsky, O.S., Spalla, O., Devreux, F., Gloter, A., Mielczarski, J.A., 2012. Formation, growth and transformation of leached layers during silicate minerals dissolution: The example of wollastonite. Geochim. Cosmochim. Acta 98, 259–281.

https://doi.org/10.1016/J.GCA.2012.09.030
Schuiling, R.D., Krijgsman, P., 2006. Enhanced weathering: An effective and cheap tool to sequester CO2. Clim. Change 74, 349–354. https://doi.org/10.1007/s10584-005-3485-y
Schuiling, R.D., Wilson, S.A., Power, L.M., 2011. Enhanced silicate weathering is not limited by silicic acid saturation. Proc. Natl. Acad. Sci. 108, E41–E41. https://doi.org/10.1073/pnas.1019024108
Scott, P.W., Critchley, S.R., Wilkinson, F.C.F., 1986. The chemistry and mineralogy of some granulated and pelletized blastfurnace slags. Mineral. Mag. 50, 141–148.
Si, C., Ma, Y., Lin, C., 2013. Red mud as a carbon sink: Variability, affecting factors and environmental significance. J. Hazard. Mater. 244–245, 54–59. https://doi.org/10.1016/j.jhazmat.2012.11.024
Song, Q., Guo, M.Z., Wang, L., Ling, T.C., 2021. Use of steel slag as sustainable construction materials: A review of accelerated carbonation treatment. Resour. Conserv. Recycl. 173, 105740. https://doi.org/10.1016/J.RESCONREC.2021.105740
Sorlini, S., Sanzeni, A., Rondi, L., 2012. Reuse of steel slag in bituminous paving mixtures. J. Hazard. Mater. 209–210, 84–91. https://doi.org/10.1016/j.jhazmat.2011.12.066
Stubbs, A.R., Paulo, C., Power, I.M., Wang, B., Zeyen, N., Wilson, S.A., 2022. Direct measurement of CO2 drawdown in mine wastes and rock powders: Implications for enhanced rock weathering. Int. J. Greenh. Gas Control 113, 103554. https://doi.org/10.1016/J.IJGGC.2021.103554
Stumm, W., Morgan, J.J., 1996. Aquatic Chemistry: Chemical Equilibria and Rates in Natural Waters, 3rd ed, Aquatic Chemistry: Chemical Equilibria and Rates in Natural Waters. John Wiley & Sons, Inc.
Tayebi-Khorami, M., Edraki, M., Corder, G., Golev, A., 2019. Re-Thinking Mining Waste through an Integrative Approach Led by Circular Economy Aspirations. Minerals 9, 286. https://doi.org/10.3390/min9050286
Thom, J.G.M., Dipple, G.M., Power, I.M., Harrison, A.L., 2013. Chrysotile dissolution rates: Implications for carbon sequestration. Appl. Geochemistry 35, 244–254. https://doi.org/10.1016/j.apgeochem.2013.04.016
Tollefson, J., 2018. Sucking carbon dioxide from air is cheaper than scientists thought [WWW Document]. URL https://www.nature.com/articles/d41586-018-05357-w (accessed 2.12.20).
Turvey, C.C., Hamilton, J.L., Wilson, S.A., 2018a. Comparison of Rietveld-compatible structureless fitting analysis methods for accurate quantification of carbon dioxide fixation in ultramafic mine tailings. Am. Mineral. 103, 1649–1662. https://doi.org/10.2138/am-2018-6515
Turvey, C.C., Wilson, S.A., Hamilton, J.L., Southam, G., 2017. Field-based accounting of CO2 sequestration in ultramafic mine wastes using portable X-ray diffraction. Am. Mineral. 102, 1302–1310. https://doi.org/10.2138/am-2017-5953
Turvey, C.C., Wilson, S.A., Hamilton, J.L., Tait, A.W., McCutcheon, J., Beinlich, A., Fallon, S.J., Dipple, G.M., Southam, G., 2018b. Hydrotalcites and hydrated Mg-carbonates as carbon sinks in serpentinite mineral wastes from the Woodsreef chrysotile mine, New South Wales, Australia: Controls on carbonate mineralogy and efficiency of CO2 air capture in mine tailings. Int. J. Greenh. Gas Control 79, 38–60. https://doi.org/10.1016/j.ijggc.2018.09.015
Ul-Hamid, A., 2018. A Beginners' Guide to Scanning Electron Microscopy, A Beginners' Guide to Scanning Electron Microscopy. https://doi.org/10.1007/978-3-319-98482-7

UNSD, 2016. United Nations Statistics Division - Environment Glossary [WWW Document]. URL https://unstats.un.org/unsd/environmentgl/gesform.asp?getitem=1178 (accessed 10.9.20).

Urbán, L., Csépli, Z., 2010. Disaster in the Ajka Red Sludge Reservoir on 04 October 2010, in: Sixth Meeting of the Conference of He Parties to the Convention on the Transboundary Effects of Industrial Accidents. MoI of Hungary.

Van Gerven, T., Cornelis, G., Vandoren, E., Vandecasteele, C., Garrabrants, A.C., Sanchez, F., Kosson, D.S., 2006. Effects of progressive carbonation on heavy metal leaching from cement-bound waste. AIChE J. 52, 826–837. https://doi.org/10.1002/AIC.10662

Vanderzee, S.S.S., Dipple, G.M., Bradshaw, P.M.D., 2019. Targeting Highly Reactive Labile Magnesium in Ultramafic Tailings for Greenhouse-Gas Offsets and Potential Tailings Stabilization at the Baptiste Deposit, Central British Columbia (NTS 093K/13, 14). Geosci. BC Summ. Act. 2018 Miner. Min. 109–118.

Wang, X., Ni, W., Li, J., Zhang, S., Hitch, M., Pascual, R., 2019. Carbonation of steel slag and gypsum for building materials and associated reaction mechanisms. Cem. Concr. Res. 125, 105893. https://doi.org/10.1016/J.CEMCONRES.2019.105893

Washbourne, C.-L., Renforth, P., Manning, D.A.C., 2012. Investigating carbonate formation in urban soils as a method for capture and storage of atmospheric carbon. Sci. Total Environ. 431, 166–175. https://doi.org/10.1016/j.scitotenv.2012.05.037

Washbourne, C.L., Lopez-Capel, E., Renforth, P., Ascough, P.L., Manning, D.A.C., 2015. Rapid removal of atmospheric CO2 by urban soils. Environ. Sci. Technol. 49, 5434–5440. https://doi.org/10.1021/es505476d

Wilcox, J., Psarras, P.C., Liguori, S., 2017. Assessment of reasonable opportunities for direct air capture. Environ. Res. Lett. 12. https://doi.org/10.1088/1748-9326/aa6de5

Wilson, S.A., Dipple, G.M., Power, I.M., Barker, S.L.L., Fallon, S.J., Southam, G., 2011. Subarctic Weathering of Mineral Wastes Provides a Sink for Atmospheric CO2. Environ. Sci. Technol. 45, 7727–7736. https://doi.org/10.1021/es202112y

Wilson, S.A., Dipple, G.M., Power, I.M., Thom, J.M., Anderson, R.G., Raudsepp, M., Gabites, J.E., Southam, G., 2009a. Carbon dioxide fixation within mine wastes of ultramafic-hosted ore deposits: Examples from the Clinton Creek and Cassiar Chrysotile deposits, Canada. Econ. Geol. 104, 95–112. https://doi.org/10.2113/gsecongeo.104.1.95

Wilson, S.A., Harrison, A.L., Dipple, G.M., Power, I.M., Barker, S.L.L., Ulrich Mayer, K., Fallon, S.J., Raudsepp, M., Southam, G., 2014. Offsetting of CO2 emissions by air capture in mine tailings at the Mount Keith Nickel Mine, Western Australia: Rates, controls and prospects for carbon neutral mining. Int. J. Greenh. Gas Control 25, 121–140. https://doi.org/10.1016/j.ijggc.2014.04.002

Wilson, S.A., Raudsepp, M., Dipple, G.M., 2009b. Quantifying carbon fixation in trace minerals from processed kimberlite: A comparative study of quantitative methods using X-ray powder diffraction data with applications to the Diavik Diamond Mine, Northwest Territories, Canada. Appl. Geochemistry 24, 2312–2331. https://doi.org/10.1016/j.apgeochem.2009.09.018

Wilson, S.A., Raudsepp, M., Dipple, G.M., 2006. Verifying and quantifying carbon fixation in minerals from serpertine-rich mine tailings using the Rietveld method with X-ray powder diffraction data. Am. Mineral. 91, 1331–1341. https://doi.org/10.2138/am.2006.2058

World Health Organization, 2014. Chrysotile Asbestos [WWW Document]. URL http://www.who.int/ipcs/assessment/public_health/chemicals_phc (accessed 12.4.20).

World Steel Association, 2021. Steel Facts [WWW Document]. URL https://www.worldsteel.org/about-steel/steel-facts.html (accessed 5.31.21).

World Steel Association, 2019. World Steel in Figures 2019.

World Steel Association, 2017. Steel Industry co-products [WWW Document]. URL https://www.worldsteel.org/publications/position-papers/co-product-position-paper.html (accessed 10.14.19).

Yang, J., Xiao, B., 2008. Development of unsintered construction materials from red mud wastes produced in the sintering alumina process. Constr. Build. Mater. 22, 2299–2307. https://doi.org/10.1016/j.conbuildmat.2007.10.005

Yildirim, I.Z., Prezzi, M., 2015. Geotechnical properties of fresh and aged basic oxygen furnace steel slag. J. Mater. Civ. Eng. 27, 1–11. https://doi.org/10.1061/(ASCE)MT.1943-5533.0001310

You, K., Lee, S.-H., Hwang, S.-H., Kim, H., Ahn, J.-W., 2011. CO₂ Sequestration via a Surface-Modified Ground Granulated Blast Furnace Slag Using NaOH Solution. Mater. Trans. 52, 1972–1976. https://doi.org/10.2320/matertrans.M2011110

Zevenhoven, R., Kavaliauskaite, I., 2004. Mineral carbonation for long-term CO2 storage: An exergy analysis. Int. J. Thermodyn. 7, 23–31.